Kirk-Othmer Encyclopedia of Chemical Technology.

INFORMATION STORAGE MATERIALS, MAGNETIC

Information can be recorded by applying a variety of principles and media. At present most information (∼95%) is still stored on paper, 3% on microfiche, and the remaining 2% by magnetic–optical–magnetooptical and semiconductor storage devices. Nevertheless, magnetic recording represents a multibillion dollar industry and is still a growing market.

In this article the main focus is magnetic recording (MR) and rather less on magnetooptic recording (MOR) (see Information storage materials, optical). Both methods are used for professional as well as for consumer applications. The various applications of magnetic recording include audio, video, or data recording. Each application has its own type of media in the form of tape, floppy, or hard disk. At present mor media are only available on hard disks. The trends in magnetic recording technology are continually increasing recording densities and storage capacity with a decreasing price per bit. General references on the subject of recording and related technologies are available (1–9).

1. Progress to Higher Densities

Since ∼1965 the increase in recording density has been by a factor of 1000. Based on this trend, an areal density of more than 300 Gbit/in.^{2} is predicted to be available in the twenty-first century (10) for the perpendicular recording mode. This prediction is based on computer simulation studies (11). Since the Intermag Conference of 1992, 10 Gbit/in.^{2} longitudinal recordings, having bit areas less than 0.1 μm^2, have been discussed (12). From a design point of view many improvements can be carried out to realize a recording system having very high bit recording (several gigabit per square inch). Development has shown drastic scale-down of the track pitch, bit-cell length, head gap, medium thickness, and head–medium spacing. Progress in track pitch and bit length for commercially available hard disk systems over time can be seen in Figure 1 (13). The respective necessary contributions from track pitch and bit cell length to realize a 1 Gbit/in.^{2} system are not yet commercialized, but have been demonstrated since 1990 (13–15).

Three key developments have led to increased density: (*1*) in 1970 a ferrite head was used together with a particulate medium having a coercivity of 28 kA/m (352 Oe) with a head–medium spacing of 430 nm, followed in 1980 by (*2*) a configuration of a plated medium (H_c = 56 kA/m), a thin-film head, and a spacing of 200 nm. In 1990 (*3*) a magnetoresistive read head combined with an inductive write head were introduced together with a sputtered medium having a Hc = 120 kA/m and a head/medium distance of 100 nm. Not only media are being developed with thin-film technologies but also film heads. The small spacing for high densities has introduced an additional field of research on protective layers and tribology.

Thin-film media are available commercially in MO-disks made by sputter technologies, metal evaporated tape (me-tape) for audio application, and electro-deposited and sputtered hard disks for data recording. The next generation of magnetic and magnetooptic recording products will all be dependent on the advances in the volume packing density of recorded information. Consequently there is not only a future for thin-film media but also for thin-film magnetic recording heads (smaller gap width and track width) based on inductive reading

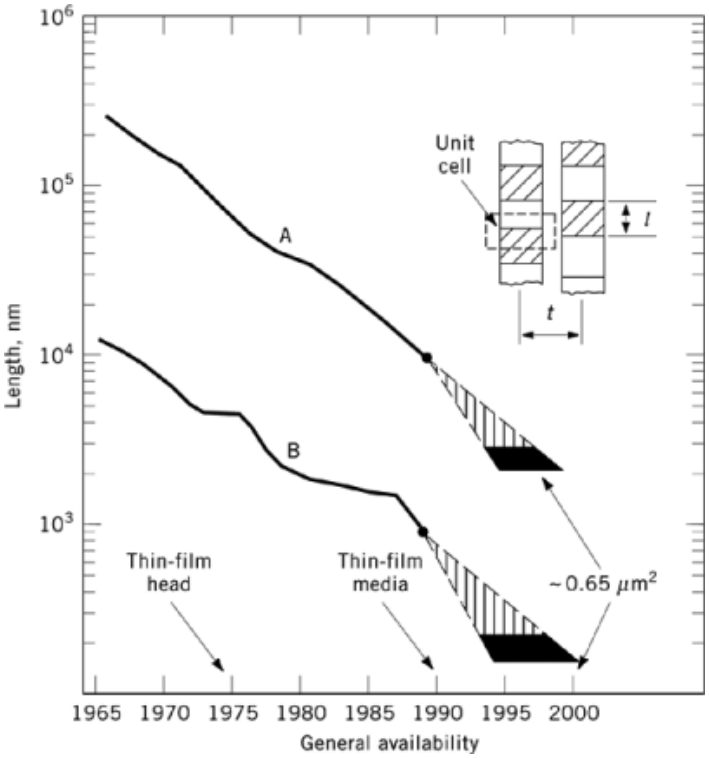

Fig. 1. Progress in track pitch, t (A) and bit cell length, l (B) implemented in disk files up to 1990. The possible changes in dimensions to obtain commercial 1 Gbit/in.^{2} (0.65 μm^2) recording are also given (13).

and writing as well as magnetoresistive sensors for the read process. Developments of multilayer deposition technologies have been the basis for new media for mor (especially for lower wavelength recording) and giant magneto resistance (gmr) layers for integration in the read head.

The increase of bit densities can easily be demonstrated by showing the bit area (ba in μm^2), which is determined by the bit cell length (bl in μm) $\times$ track width(tw in μm), for various (commercial) recording systems. In the case of video Hi8 pal (long play) the $ba = 3.4\ \mu m^2$ ($bl = 0.2\ \mu m \times tw = 17\ \mu m$), Hi8 ntsc (long play) $ba = 2.5\ \mu m^2$ ($bl = 0.25\ \mu m \times tw = 10\ \mu m$), for hdtv (experimental Philips system) $ba = 2.5\ \mu m^2$ ($bl = 0.25\ \mu m \times tw = 10\ \mu m$), hdtv (Philips research) $ba = 1.25\ \mu m^2$ ($bl = 0.25\ \mu m \times tw = 5\ \mu m$), and digital audio tape (dat) $ba = 4.2\ \mu m^2$ ($bl = 0.33\ \mu m \times tw = 14\ \mu m$).

It has been demonstrated by IBM (13–15) that for 1.18 Gbit/in.^{2} a hard disk system for longitudinal recording the $ba = 0.76\ \mu m^2$. Here the bit cell length is 0.19 μm and the track width 4 μm. Hitachi has reported an areal bit density of 2 Gbit/in.^{2} with $bl = 0.21\ \mu m \times tw = 1.5\ \mu m$ (16).

With respect to recording systems, modern developments and knowledge of electronics, mechanics, control engineering, etc, have also led to an increase of the densities in actual commercial systems. Thin-film technologies have changed the media and heads, but for increasing the density other aspects such as the encoding of information are also important and have been changed from analogue to digital. Although digital encoding has already been successfully applied in data recording there is also a trend to use this recording method for video (hdtv) and audio applications (dcc), because errors can be corrected dynamically. Reconstruction of the original information can be carried out very precisely.

2. Magnetic Properties of Recording Materials

The relation between the three important values for a magnetic material is shown in equation 1:

$$B = \mu_0 \ (H + M)$$

where B is the magnetic induction or flux density generated by a magnetic field H. The magnetic induction also consists of a contribution from the magnetization M. The B in free space is $\mu_0 H$ whereas the contribution from the M of the material is $\mu_0 M$. The vector sum of both is thus $B = \mu_0(H + M)$ in which μ_0 is the permeability in free space ($\mu_0 = 4\pi \times 10^{-7}$ hy/m). The relative permeability in a material is defined as μ_r and given by $\mu_r = \mu/\mu_0$. A classification for the various types of magnetic materials is given by their susceptibility ($\chi = M/H$) or permeability ($\mu = B/H$). Materials are diamagnetic if χ is small and negative ($\sim -10^{-5}$); another group also having a small but positive χ value ($\sim 10^{-4}$) are called paramagnetic. The most important materials for recording can be divided into ferromagnetic materials like Fe, Co, Ni ($\chi = 50$ to 10^4), and ferrimagnetic materials, eg, γ-Fe_2O_3, ferrites. The ferrimagnetic materials also have similar macroscopic behavior to that of the ferromagnets. They both show a spontaneous magnetic moment which means that the magnetization persists even without an applied field. Only these materials have magnetizations large enough for applications. The media used for recording are termed magnetically hard; in comparison with permanent magnet materials it would be better to define them as semihard. The magnetic head materials have the properties of soft magnetic materials. Consequently their properties are very different.

2.1. Intrinsic and Extrinsic Properties

The materials Fe, Co, and Ni and their alloys and oxides are mostly used for recording applications materials. Their magnetic properties are described by intrinsic and extrinsic parameters. The intrinsic properties (saturation magnetization, M_s, magnetocrystalline anisotropy, K, Curie temperature, T_C, and the magnetostriction, λ_s) are determined by the type and number of atoms, their arrangement in the crystal structure and their temperature. The extrinsic properties (remanent magnetization M_r, coercivity H_c, and permeability μ) can also be influenced by the size and shape of the magnetic material and its (magnetic) history. Consequently, in the case of thin-film media, microstructure and morphology play a key role in determining extrinsic properties.

Figure 2 shows the two hysteresis loops for a medium and a head material. The coercivity, H_c, the saturation magnetization, M_s or induction, B_s, remanent magnetization, M_r or induction, B_r, and the permeability, μ, differ for the two materials.

If a very high field is applied the magnetization can reach its saturated state in which all the magnetic dipoles are aligned in the direction of the field. If the magnetic field is switched off, the remanent magnetization M_r is left. If the M (or B) is then reduced to zero, a special field strength, the coercivity, H_c, is required.

The hysteresis loop, in general, supplies information about the magnetic properties such as H_c, M_s, M_r, preferred direction of the magnetization or anisotropy, and it can even give some idea about the magnetization reversal process involved. In general, recording media requirements are high coercivity, high remanent magnetization, high squareness ($S = M_r/M_s$) of the hysteresis loop, and low noise.

The properties for head materials can be summarized as large saturation magnetization for producing a large gap field, high permeability at all frequencies in order to ensure high efficiency, small coercivity with low hysteresis loss, low magnetostriction for obtaining low–medium contact noise, and small but not zero magnetic anisotropy to suppress the domain noise. To ensure good reliability and a long operating time, the head materials must exhibit a good thermal stability and a high resistance to wear and corrosion. The choice of materials and preparation technologies are the tools for tailoring head and medium properties.

The transition temperature at which ferromagnetic behavior of a material changes into paramagnetic is called the Curie temperature (T_C for Co, Fe, and Ni, respectively, is 1130, 770, and 358°C). At T_C the μ

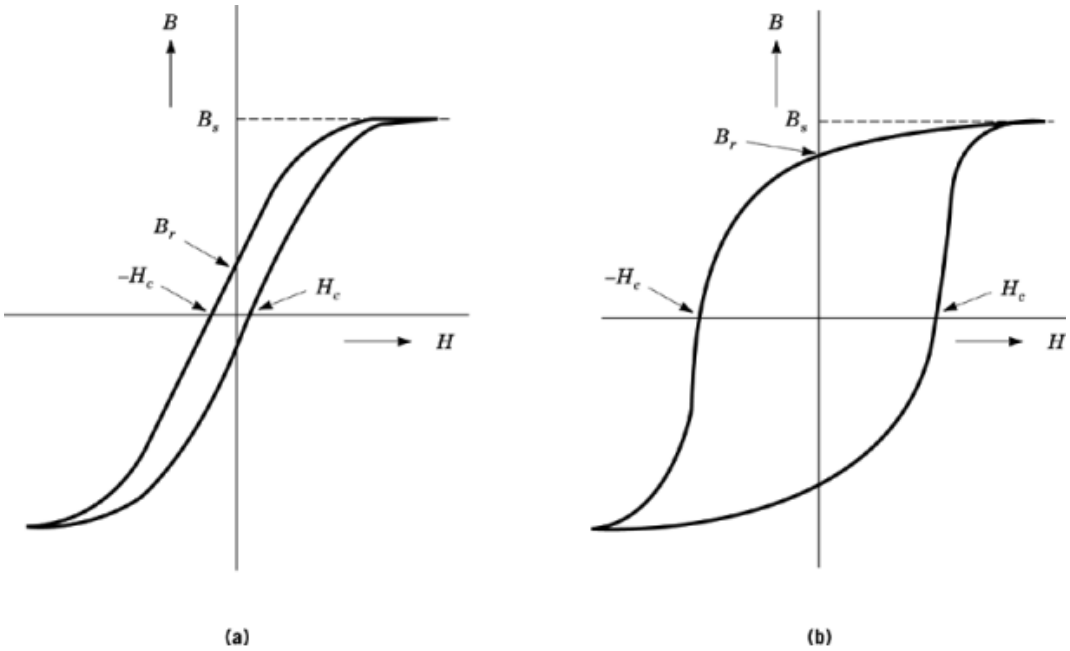

Fig. 2. Basic hysteresis properties for (**a**) a recording head and for (**b**) a magnetic medium. See text.

decreases drastically and the H_c and M_r become zero. The saturation magnetostriction (λ_s) can be defined as the fractional change in length if the sample is saturated from the demagnetized state along the field direction. The λ_s is different for isotropic and anisotropic materials. The field-induced magnetostriction is the variation of λ with H or B and is an important parameter for magnetic head materials.

Many magnetic materials show preferential directions for the alignment of the magnetization. These directions are energetically favorable and are called easy axes. The energetically unfavorable directions are known as hard axes and are rotated through 90° from the easy axis. When a material has only one easy axis the material is said to have uniaxial magnetic anisotropy. Multiaxial anisotropy occurs in some materials but is less common. The formation of uniaxial anisotropy is not only originated by the crystal symmetry but also by preferential (poly-) crystallite orientation (texture), shape, and size of the sample and stresses.

The strength of the anisotropy determines the difficulty of rotating the magnetization direction away from its stable alignment with the preferred axis and is thus an influencing factor for the magnitude of the coercivity. Anisotropy can also be induced by applying a strong magnetic field during preparation. In the case of multilayers for magnetooptic recording the so-called interface anisotropy (related to the surface anisotropy and strain) is also of great influence. The shape anisotropy in certain directions depends on the dimensions of the sample and varies with the shape (sphere, elongated particle, thin film). This anisotropy is inherently uniaxial.

Magnetocrystalline anisotropy arises from exchange forces within the crystal lattice and is therefore an intrinsic material parameter in contrast to the shape anisotropy. Materials do have crystal anisotropy if the magnetic moments prefer to lie along special crystallographic axes. This preferential direction of the magnetization leads to a lower energy. These anisotropy direction(s) are different for the various materials used. Easy axes can be found for Fe (bcc): <100>; Ni (fcc): <111> and Co (hcp): [1000]. The hard axes are, respectively, <111>, <100>, and [1010]. The magnitude of the first-order crystal anisotropy (K_1) at room temperature for Co is the largest (Co: $10\times$ Fe). The magnetocrystalline anisotropy is sensitive to temperature

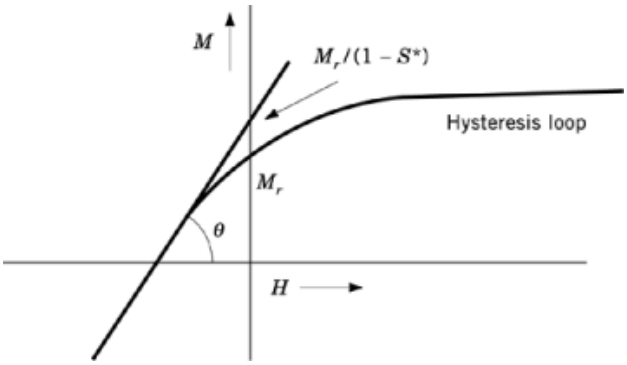

Fig. 3. Williams-Comstock construction for defining S^*.

and stress and can undergo irreversible changes if the site occupancy of the ions changes. Last but not least the strain anisotropy can play a significant role in the total anisotropy. It can be caused by stresses in magnetostrictive materials. The total anisotropy in a material is the sum of the acting anisotropies.

2.2. Switching-Field Distribution

Both M_r and H_c have a strong relation with the recording process. M_r determines the maximum output signal of a recording medium and hence the signal-to-noise ratio. H_c ascertains how easily data can be recorded and erased or changed, but it also determines the maximum head field. On the other hand it also controls the ease with which data can be destroyed, eg, by stray fields. The lower the H_c, the more sensitive the medium is to all kinds of fields. In this way, H_c influences the noise level as well. The squareness ratio S ($= M_r/M_s$) can also be derived from the hysteresis loop. A high value means that a large part of the magnetization is preserved, which is essential for recording.

The slope of the hysteresis loop in H_c is also an important parameter. From this slope, the parameter S^* can be derived (17). In Figure 3 a part of the hysteresis loop (M as a function of the applied field H) is given. The point at which M is constant as the function of the applied field is defined as saturation magnetization (M_s). From the slope at H_c can be written $\tan\theta = M_r/H_c = 1/(1 - S^*)$ or $dM/dH = M_r/H_c(1 - S^*)$. Thus the S^* is defined in relation to the slope of the loop at H_c. In the case of longitudinal recording experimental data have shown that there is a connection between S^* and recording parameters (18, 19). Although S^* is normally used as a switching field distribution (sfd) parameter, it is not always suitable. The sfd can be seen as a distribution function of the number of units reversing at a certain field. For a particulate medium without collective behavior, this function is closely related to the particle size distribution, as differently sized and shaped particles reverse at different fields. Of course the shape, orientation, and interaction between particles influence the sfd as well. Media with a high H_c and a small sfd are more suitable for high density recording (20) because the distribution of the switching fields is very small. An alternative definition is sfd $= \Delta H/H_c$. In this case the ΔH is the full width at half height of the differentiated loop *(dM/dH)*.

The micromagnetic structure is directly related to the microstructure and chemical inhomogenities in the layer. The materials used and the deposition technology as well as the parameters play an important role. Thin-film growth, nucleation processes in relation to the deposition parameters, are very important for understanding the thin film microstructure. The relationships between sfd and recording properties are not necessarily valid for media with perpendicular anisotropy as the demagnetizing field can be more important than sfd.

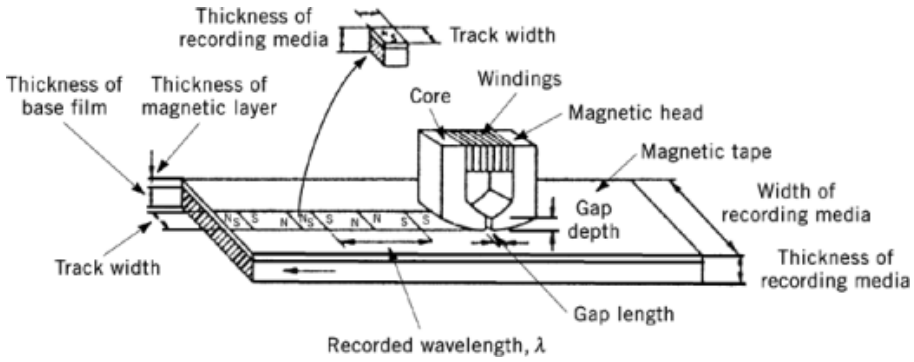

Fig. 4. Written bits in the longitudinal recording mode (LMR). Shortest recorded wavelength is $\lambda_m/2$.

3. Magnetic Recording

There are two modes of magnetic recording dependent on the direction of the magnetization (magnetic anisotropy) namely longitudinal (LMR) and perpendicular magnetic recording (PMR). In the former the magnetic anisotropy lies in the plane of the medium, and in the case of pmr the anisotropy is directed parallel to the medium normal. Magnetooptic recording (MOR) also requires a perpendicular magnetic anisotropy.

Modern recording technologies are based on digital signal processing, even for audio and video recording. Digital technologies provide a much lower signal-to-noise ratio, comfort of error detection, and correction and integration of large-scale integration (LSI) circuits technology. The input data may be either analogue (audio, video; using an a-d converter) or digital (computer data). Examples are the minidisc and dcc (digital compact cassette) for audio application and the not yet commercialized HDTV digital VTR.

3.1. Longitudinal Recording

The principles of LMR are given in Figure 4. High density recording depends on shortening the recording wavelengths and also narrowing the track width. The basic recording principles are described in detail in the literature (1–9).

The digital storage of bits in a moving medium beneath a soft magnetic head can be achieved by a current pulse in the recording head. The magnetic flux associated with the writing current travels the magnetic circuit of the head. The recording medium is in contact with or at a small distance from the gap of the magnetic head. The gap fringe flux penetrates the medium and magnetizes small volumes of the material. In the case of longitudinal recording the horizontal fringing field component is the most important one. From analytical models and experimental data it is concluded that this field should be several times the value of the coercive field of the medium (1, 2, 4). The bit size area (bit length $\times$ track width) should be small for high density recording and the transition length (magnetization reversal) as sharp as possible. The change of the head current from one polarity to another produces a magnetization that is not spatially sharp but varies over a distance from one direction to the opposite one. The transition length in longitudinal recording is mainly determined by the head field gradient and the demagnetizing fields generated by the magnetostatic fields of the transition itself and the switching field distribution of the magnetic units in the medium.

A principle configuration of the recording geometry is given in Figure 5. A ring head is used which operates on a head–medium spacing d from the media in motion. The gap length of the head is g, the magnetic thickness δ of the recording medium (in the case of thin hard disk media δ is equal to the film thickness, in the case of thick magnetic particle tape δ is smaller than the coating thickness), and the

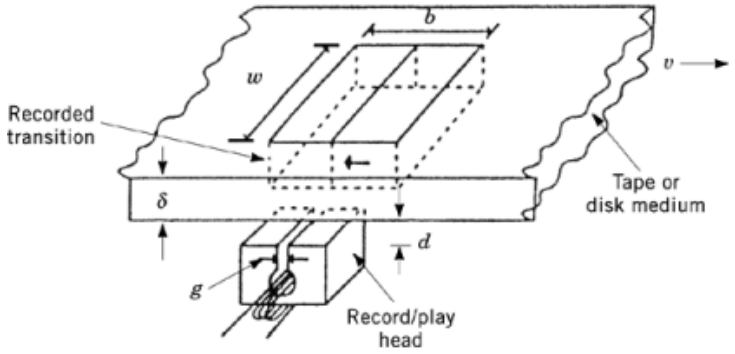

Fig. 5. Basic recording parameters for a medium bit cell and head (7).

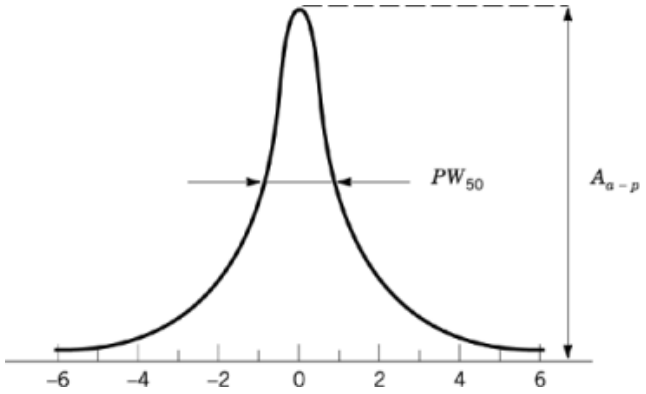

Fig. 6. Output pulse from reading a transition in the longitudinal recording mode.

recorded bit cell size is b with a track width w. A bit cell is defined as an alternative distance between recorded transitions. The bit cell area as recorded has the dimension $w \times b$. The transition length is an important factor for discussing the limitations for the recording density. The transition width a is given by equation 2 where M_r = remanent magnetization, δ = layer thickness, d = head − to − medium spacing, Q = a value related to the field gradient of an inductive head (∼0.75), and H_c = medium coercivity (17).

$$a \cong \left[\{4M_r \cdot \delta\,(d + \delta/2)\} / (Q \cdot H_c)\right]^{\frac{1}{2}}$$

For a small transition width, H_c should be large in relation to $M_r \cdot \delta$ (remanence thickness product) and d as small as possible (contact). The stored bit (transition) can be read by the head due to the flux changes in the head which gives an induced voltage. The output voltage is shaped as in Figure 6. One of the models for the shape of the magnetization transition which is often used is the arctangent model (17) described by equation 3. This model describes the recorded magnetization in the x direction (longitudinal) in response to a step function change in the write head current. The arctangent parameter, a, is inversely proportional to the maximum slope of the transition. The isolated output voltage pulse is given in Figure 6.

$$M(x) = 2/\pi M_r \arctan(x/a)$$

Narrow transitions (small a) yield large peak voltages (A_{a--p}) and narrow pulse shapes (PW_{50}). The width at half height is given by equation 4 where g = gap length head, d = head − to − medium spacing, a = transition width, and δ = layer thickness (17). A small PW_{50} gives a better resolution without interference from neighboring transitions and a higher read voltage.

$$PW_{50} \cong \left[g^2 + 4\,(d+a)\;(d+a+\delta)\right]^{\frac{1}{2}}$$

3.2. Medium Noise

In magnetic recording systems three types of noise must be considered: medium, head, and electronic noise. Medium noise is the most important factor influencing the performance of the recording system. Local structural and chemical variations in the medium cause distortions in the magnetization pattern resulting in noise in the signal. The magnitude of noise in particulate medium (CrO_2, γ-Fe_2O_3) is determined by the properties of the individual particles and the relatively weak magnetostatic interactions between the particles. The packing density (ratio between a magnetic and nonmagnetic material) is the key factor for this noise. In general smaller particles have a statistical reduction of noise. This rule is valid if the medium does not have exchange coupling and small effects of magnetostatic interaction. However, very small particles give a continuous decrease of coercivity until the particles become then superparamagnetic. New materials having higher switching energies have been developed either with higher coercivities or higher magnetization. The density for γ-Fe_2O_3 particles with a particle length of 1 μm is about $10_{11}/mm^3$. Cobalt-modified γ-Fe_2O_3 (length 0.5 μm) increases density by a factor of 10. The recently developed metallic Fe particles (length 0.25 μm) have a density of 10^{13}. Smaller particles having higher switching fields (higher H_c and/or M_s) are being developed.

In metal thin-film media consisting of very small grains, a 10 × larger grain − packing density has been achieved but individual grains are not single acting magnetic particles. Depending on microstructural aspects the contribution of the exchange coupling and the magnetostatic interaction must be taken into account. The intergranular distance is only very small compared with that of the particulate medium. Switching of clusters of grains is more obvious. This results in irregular magnetization patterns in the written transition and therefore to noise in the output signal.

Higher densities and lower noise consequently results from smaller bits containing crystallites with smaller sizes. As an example, a one-bit cell in the Co-based medium used for the IBM 1.19 Gbit/in.^{2} demonstration disk (13) consists of about 1900 grains with a grain size of about 20 nm. Consequently, for a 10 Gbit/in.^{2} thin-film media a grain size of about 10 nm is necessary (smaller grain size is not possible due to the superparamagnetic limit). In this case there will be about 600 grains in a one-bit area.

3.3. Perpendicular Recording

In the case of perpendicular recording the easy axis of the magnetization is perpendicular to the medium (Fig. 7). The most important reason for developing the perpendicular mode of recording is that in the high density area the transition length becomes more and more important. This mode of recording has been studied for application since 1975 by discussing the circular magnetization mode and the technology for preparing a Co–Cr film with a perpendicular anisotropy (21). Since that time Co–Cr has been the most promising material for medium application in perpendicular recording, although other media materials such as Co–O and Ba ferrite films and particles are still under development. Commercial use was announced but not realized in 1989 (22) when Censtor Corp. started working in conjunction with Northern Telecom in the United States. Current strategies about hard-disk contact or quasicontact perpendicular recording have been discussed (23). Research activities and published results indicate no specific scientific problems preventing the use of perpendicular recording systems. Perhaps there are commercial reasons for its nonuse such as the continuous improvement

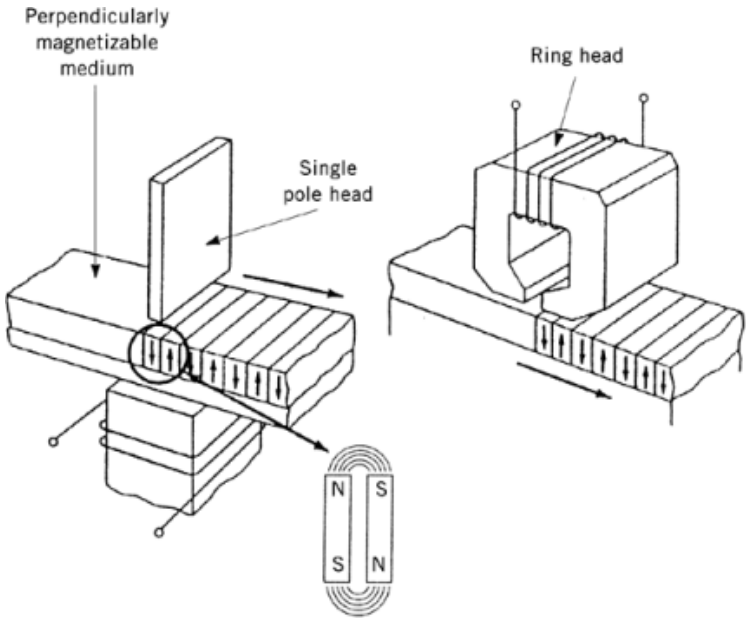

Fig. 7. Principle perpendicular recording for a ring head and a head consisting of a single pole with an auxiliary pole.

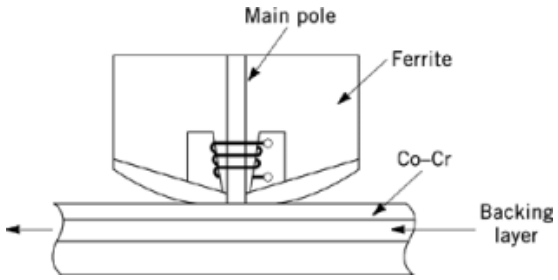

Fig. 8. The main-pole driven head in combination with a Co–Cr/Ni–Fe double-layer medium for perpendicular recording.

of the longitudinal recording technology, eg, the Gbit/in.^{2} demonstrations by IBM in the United States (15) and Hitachi in Japan (16).

Nevertheless, in spite of lack of commercial success the perpendicular mode has stimulated the other modes of recording and presents many new scientific questions that have to be solved concerning new specific heads, contact between head and medium, and the development of suitable thin-film media. The total concept of this type of recording can only be accomplished as a complete success if the media and head development take place as a unified project. For instance, a combination of a perpendicular head and a so-called double-layer medium, as shown in Figure 8, in which the bottom (backing) layer NiFe was prepared as a soft magnetic layer with a top layer of Co–Cr, has been used for very high density recording studies (25).

A single-layer medium can also be used in combination with a very narrow gap ring head having a high saturation induction core (26). It was clear from the research that the proper high density recording conditions are much more severe for the single-layer medium. Much of the research in the field of perpendicular recording is concentrated in Japan.

3.4. Demagnetization

The internal microstructure as well as the macroscopic shape can influence the internal magnetizing field. In the case of PMR and MOR the anisotropy must be perpendicular, which means that the highest demagnetization field is directed opposite to the magnetization of the sample. This means that the anisotropy energy in the perpendicular direction should be larger than the demagnetizing energy for the perpendicular direction of the magnetization.

In Figure 9 the initial states of the magnetization are given for the two recording modes. In both cases two written bits with their directions of magnetization opposite and parallel to the anisotropy direction are drawn. In Figure 9**a** the transitions with uniform magnetization and zero width can be seen. The corresponding magnetizations and demagnetizing fields are shown in Figure 9**b**. In contrast to the longitudinal mode, the H_{d} in the perpendicular mode vanishes at the transition. As a consequence the longitudinal transition will be spread out, in contrast to the perpendicular transition, which is sharpened (see Fig. 9**c**). In the case of very high density transition recording this principle shows the advantage for the perpendicular mode, but magnetic recording is more than just considering the transition. The recorded bits for lmr media are shown in Figure 4. For very high densities the written bit is enlarged separately in the figure; as the bit length ($\lambda/2$) approaches zero the H_{dx} (see also Fig. 9) in the direction of the media motion approaches one, whereas the transition (M_{x}) becomes unsharp. At very high bit densities, the longitudinal media is thin (10–50 nm) and the perpendicular media can still be between 50–250 nm. The demagnetizing field also plays an important role, especially in the case where there are media with perpendicular anisotropies. For a thin continuous layer, having no other anisotropy sources, the magnetization prefers to lie parallel to the film plane, being the state of minimum energy. In the case of Co–Cr having perpendicular anisotropy there is, in principle, a competition between the uniaxial anisotropy of a hexagonal structure and the demagnetizing energy of the thin film. In the case of magnetically separated Co–Cr columns (particulate morphology) then also the shape anisotropy contributes to the perpendicular anisotropy.

Most calculations on perpendicular films start at a state of uniform perpendicular magnetization, and from this a so-called quality factor can be derived as $Q = 2K_1/\mu_0 M_s$. In the case of a uniform magnetized layer with $Q > 1$, the perpendicular axis is thus the direction of the preferred magnetization. However, the state of uniform perpendicular magnetization is quite unusual. Either the magnetization of the layer is split up into domains by the demagnetizing forces, or the layer is in the recorded state. In the latter case, shape anisotropy of a thin film loses its meaning and the demagnetizing energy density (E_{d}) of a stripe-domain structure (27) must be considered. If the domain width d is smaller than the layer thickness δ, then $E_d = 0.136\ \mu_0 d/\delta M_s$. The condition for stable perpendicular magnetization ($K_1 > E_d$) expressed in Q becomes $Q = 0.27d/\delta$. If a Co–Cr layer with typical parameter values is considered ($M_s = 400$ kA/m and $\delta = d = 1\ \mu$m) and $Q > 0.27$. This is much more stringent than in the previous case where $Q > 1$. This simple example shows that a substantial perpendicular magnetization may be expected even if $Q < 1$.

3.5. Magnetooptic Recording

Magnetooptic recording is the oldest mode of perpendicular recording; it was demonstrated in the literature in 1957 using a medium MnBi having a perpendicular anisotropy (28). This mode of recording combines the advantages of optical and magnetic recording. The number of commercial systems is growing. The minidisk is a good example for using MO-recording technologies for consumer applications. The status and future of MO-disk drive technologies is discussed in Reference 29.

As can be seen in Figure 10 (30) reversed domains are formed with a focused laser spot (diameter $< 1\ \mu$m) in a perpendicular magnetically saturated disk. Writing is based on the thermomagnetic writing process which means that the magnetization reversal can be achieved by the demagnetizing field or by an applied field, heating the material above its Curie temperature. In threshold writing advantage is taken of the property of some

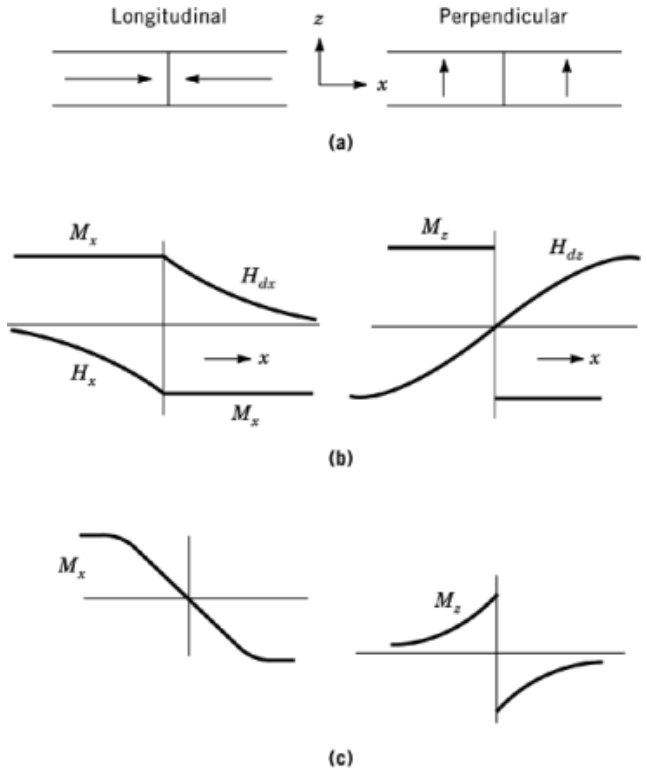

Fig. 9. The relation of an LMR and PMR transition: (**a**) initial state of magnetization; (**b**) the magnetization and corresponding demagnetization fields of **a**; and (**c**) the resultant magnetization of the different modes.

materials that the coercivity decreases strongly with increasing temperature. In this case the magnetization reversal takes place if the applied field plus the demagnetizing field is larger than the H_c during (local) heating.

Pulsed diode laser beam has been used for writing at a wavelength of 800 nm and 10 mW/100 ns. The disk is rotated at a frequency of 37 Hz. The external applied field perpendicular to the medium is lower than the H_c of the medium at room temperature in order to limit the switching to the heated spot only. The same laser as for the write operation is used for reading but at a lower power level. Magnetooptical read-out is based on the fact that a change in polarization direction occurs when linearly polarized light is reflected from a magnetic surface (polar Kerr effect). The sign and magnitude of the Kerr angle (θ_K) depend on the direction and magnitude of the magnetization vector with respect to the propagation direction of the light. The polarization vector of the written domains in Figure 1 (magnetization up) are rotated with $-\theta_K$ while the rest of the saturated disk is rotated in the opposite direction ($+\theta_K$).

Erasing of the information can be realized by heating the film with a laser beam while reversing the applied field. This is one of the limitations of mo because it slows down the data rate by a factor of ~ 2. New media designs (exchange coupled magnetic films) are proposed for realizing direct overwrite by modulating the laser power during the write process (31).

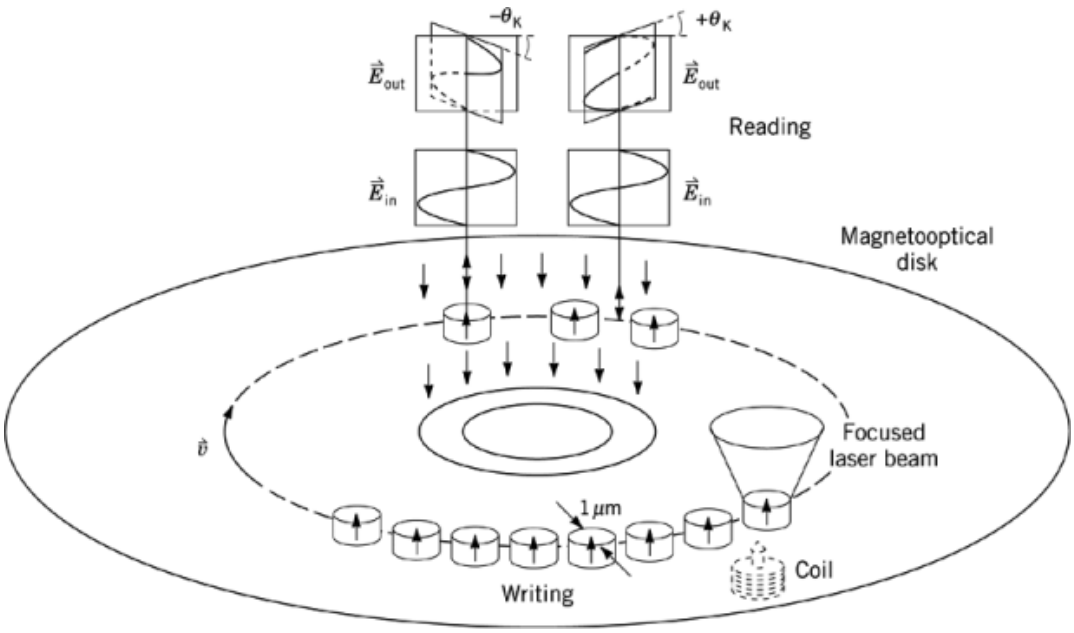

Fig. 10. Written bits in magnetooptic medium (30).

4. Magnetization Reversal Mechanisms

The reversal of the magnetization is a basic principle of magnetic recording. Magnetization in a material can be reversed by applying a field, and finally the whole material will be saturated in a direction parallel to the field. The two different states of + and − magnetization is the basic idea for digital information storage. The mode of magnetization reversal depends on the material and its size and shape. The two principle methods for reversing the magnetization are rotation and domain-wall motion. Both modes can be examined in terms of energy considerations. The coherent rotation mechanism and the incoherent rotation mechanism only occur in single-domain particles. A particle is single domain below certain dimensions. Above a critical radius a domain wall can exist and the reversal takes place by domain-wall motion.

In the coherent rotation mode the atomic spins remain parallel during the reversal process and may apply only for very small particles. If the particle size increases, incoherent switching mechanisms like curling, buckling, and fanning are used. Magnetic thin films with a polycrystalline structure are strongly exchange coupled and consequently their magnetization reversal takes place by domain-wall motion. In the case of high density recording low noise is a requirement (particulate reversal behavior is necessary for a sharp transition) and certain magnetic properties (high H_c and M_r). By tailoring the microstructural properties, continuous thin films are also promising candidates for actual and future applications.

4.1. Switching of a Single-Domain Particle

If an isolated ferromagnetic particle is considered, then the magnetization reversal depends on the dimension of this particle. For recording the so-called single-domain particles dispersed in the medium are most important to deal with. Single-domain behavior can be described by classical nucleation theory (32). A so-called Stoner-Wohlfarth particle is characterized by a uniaxial anisotropy K, the applied field H, and the direction of the magnetization due to H is M. The angle α is between H and the easy axis; θ is the angle between M and H.

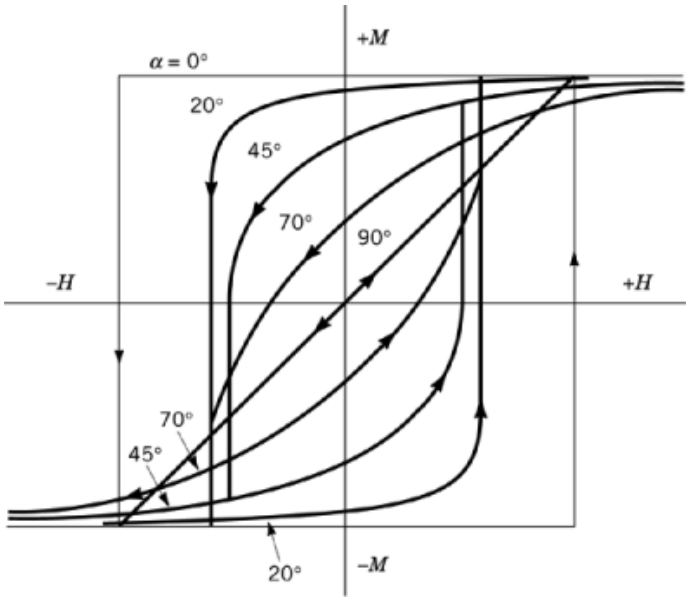

Fig. 11. Magnetization M in the direction of the applied field H for various applied-field angles with the easy axis (33).

The anisotropy energy E_a can be expressed as $-K\sin\alpha$. If M is oriented at an angle $(\alpha - \theta)$ with the easy axis this gives a torque of $2K\sin(\alpha - \theta\cos(\alpha - \theta)))$. The torque produced by an applied field, H, is $\mu_0 HM_s \sin\theta$. The equilibrium is given by $2K\sin(\alpha - \theta)\cos(\alpha - \theta) = \mu_0 HM\sin\theta$. The M–H loops with the M component in the direction of the applied field for rotation unison are given in Figure 11 for various angles between the long axis of the particle and the direction of the applied field.

At a field H_s at which the particle is saturated perpendicular to the easy axis $(\alpha = 90)$, $H_s = 2K/\mu_0 M_s$. This field can be defined as the anisotropy field H_k. Applying a field in opposite direction in the easy axis, a completely reversible change of M, by pure rotation, occurs without hysteresis. On the contrary, if a field is applied antiparallel to the anisotropy axis the particle switches irreversibly (no rotation) only after applying a field greater than $2K/\mu_0 M_s$.

This critical field called coercivity H_c or switching field H_s, is also equal to H_k. If a field is applied in between 0 and 90° the coercivity varies from maximum to zero. In the case of this special example the applied field $H_a = H_s = H_c = H_k$. Based on the classical theory, Stoner-Wohlfarth (33) considered the rotation unison for noninteracted, randomly oriented, elongated particles. The anisotropic axis can be due to the shape anisotropy (depending on the size and shape of the particle) or to the crystalline anisotropy. In the prolate ellipsoids b is the short axis and a the longest axis. The demagnetizing factors are N_a (in the easy direction) and N_b. The demagnetizing fields can then be calculated by $H_{da} = -N_a M_s$, and $H_{db} = -N_b M_s$. The shape anisotropy field is $H_d = (N_a - N_b)M_s$. Then the switching field $H_s = H_d = (N_a - N_b)M_s$.

If there is a crystal anisotropy, with the easy axis parallel to the shape-anisotropy axis of the particle, the total anisotropy is $H_a = H_{a,\text{shape}} + H_{a,\text{crystal}}$ and the total switching field is $H_s = (N_a - N_b)M_s + 2K_1/\mu_0 M_s (K_1 = \text{crystal anisotropy constant})$. In the case of practical materials it became clear that H_s was much lower than predicted by the Stoner-Wohlfarth theory. Therefore the incoherent rotation modes (fanning, curling, buckling) have been explored. The aim of the chain of spheres reversal mode (34) was to give a more realistic picture for an elongated particle used in a particulate recording medium. This reduced the switching field drastically. Furthermore, curling has been introduced as another nonuniform rotation process. In this reversal mode the particle is assumed to be spheroid or an infinite cylinder with its long axis in

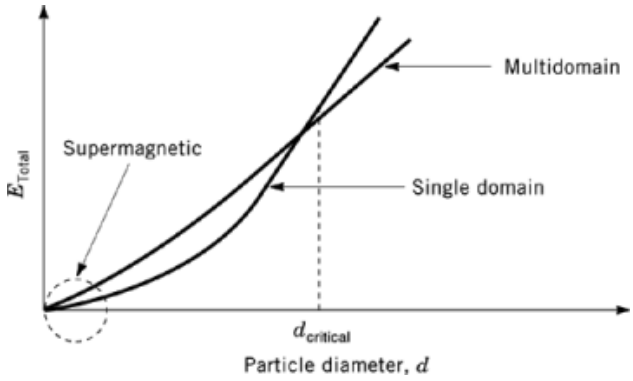

Fig. 12. Total energy vs particle diameter for single- and multidomain particles.

the field direction. An applied field parallel and opposite to the long direction, the nucleation field, is given by

$$H_n = -2K_i/\mu_0 + N_a M_s - 2\pi kA/\mu_0 M_s * 1/R$$

Here K_i is the intrinsic anisotropy constant due to the crystalline anisotropy. After the demagnetization in the longest direction, k is the shape-dependent constant (for an infinite cylinder $k = 1.38$), A is the exchange constant, and R the particle radius. An infinite cylinder with only shape anisotropy gives $H_n = -6.8A/\mu_0 M_s * 1/R$.

Isolated particles, ie, noninteracting particles, are not realistic in recording media. The magnetostatic interaction of the particles should be taken into account. Although the packing densities are not high there is still cluster forming and particles at very close distances. These kinds of effects and also, for instance, the particle-size distributions, influence the switching fields and coercivity behavior.

Below a critical size the particle becomes superparamagnetic; in other words the thermal activation energy kT exceeds the particle anisotropy energy barrier. A typical length of such a particle is smaller than 10 nm and is of course strongly dependent on the material and its shape. The reversal of the magnetization in this type of particle is the result of thermal motion.

Beside single-domain particles, multidomain particles also exist. The distribution in domains lowers the magnetostatic energy but increases the exchange energy caused by the domain walls. The reversal in such particles mainly takes place by domain-wall motion. This kind of reversal mechanism influences the coercivity. Figure 12 gives the relation between the total energy and the particle diameter. The crossing of the curve shows the critical diameter where the particle changes from single- to multidomain. At very low energies superparamagnetic particles can be found.

In Figure 13 the relation between the intrinsic coercivity H_{ci} and the particle diameter d is given. The figure is based on a described model (35). The maximum is found around the critical particle diameter. In general the particle diameter and size is not very well defined. For the multidomain particles ($d > d_{critical}$) the H_{ci} is smaller than the intrinsic anisotropy field of the particle. Nucleation effects cause a decrease in H_c as the d increases. This behavior is understood only qualitatively; for a full description see Reference 36. Low noise media should consist of single-domain particles; reversal by domain walls is slow and introduces noise.

4.2. Reversal Mechanism in Thin Films

The ideal magnetic structure for magnetic recording medium consisting of a polycrystalline microstructure is that a crystallite reversed its magnetization by rotation and not by domain-wall motion. In other words, for high density recording the crystallites should act as independent single-domain particles consequently without

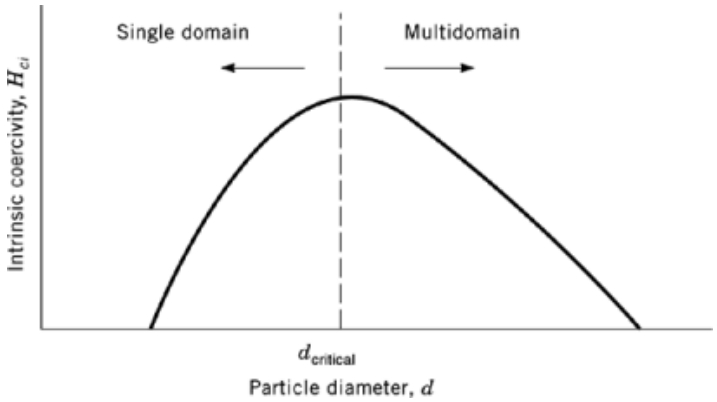

Fig. 13. The intrinsic coercivity H_{ci} vs the particle diameter for single- and multidomain particles (35).

exchange coupling, but depending on the particle distance still with magnetostatic coupling. In practice the thin films possess a wide distribution of grain size, and not all crystallites are completely separated from each other. This influences the reversal behavior.

There are two main models from the microstructural point of view, namely the particulate and the continuous microstructural model. In the first one the crystals that are formed during film deposition are believed to interact only through magnetostatic interaction. No exchange force acts over the column boundaries due to physical separation. In the continuous model the reversal mechanism is thought to take place by Bloch walls as in stripe domains, hindered by the column boundaries which can increase the coercivity of the medium. This has been studied at length for Co–Cr films having a perpendicular anisotropy (37). Several methods have been used for studying the magnetization process by experiments based on microscopic observations like magnetooptical Kerr microscopy, bitter technique, colloid-sem method, neutron depolarization, Lorentz electron microscopy, and magnetic force microscopy on the one hand, but on the other macroscopic analysis has also been applied by studying the various parameters of the hysteresis loop (measured with a vibrating sample magnetometer) and also the angular dependence of the applied field. Several groups have conducted research in the field of micromagnetic simulations. Studying the intrinsic domain structures can contribute to the understanding of the reversal process involved.

4.3. Hysteresis Loop and Reversal Process in Thin-Film Media

Materials used as storage media should have a nonequilibrium behavior which can be designated as a memory. For a magnetic recording medium this behavior is represented by hysteresis loops. The transition between two states of $+M_r$ and $-M_r$ represent the presence of information. Due to the Weiss domain theory the atomic moments in a ferromagnetic material are ordered. The difference between the demagnetized and the magnetized state is due to the dimensions and the number of domains having opposite directions of magnetization.

In the transition from the demagnetized state ($H = 0$; $M = 0$) to saturation (H = large; $M = M_s$), small domains (aligned favorably with the field) grow in the direction of the field (wall motion). Increasing the field another reversal mechanism is relevant, namely the rotation of the magnetization into the easy axis. At very high fields the moments lying in the direction of the easy axis, which is close to the applied field, are coherently rotated in the direction of the field. The final state of the material is a single domain (if the applied field is sufficiently high). In this description the magnetization is reversed mainly by domain-wall motion which means movement and bowing of the wall. Bowing of the wall at low fields is a reversible process,

but irreversible bowing can occur if the wall is sufficiently deformed. It can be stacked by pinning sites. Many microstructural properties can influence the domain-wall motion such as grain boundaries, defects, chemical inhomogeneties, magnetostriction, etc. Magnetization reversal by domain-wall motion can also be the origin of very high coercivities.

Such materials cannot be used for low noise recording because for sharp transitions (no zigzag configuration) it is necessary to avoid exchange coupling between the magnetic units (grains, columns, particles) and to lower the magnetostatic interactions. Furthermore, reversal by domain-wall motion, even in a real particulate medium, acts as a noise source. Consequently small nonexchange coupled single-domain grains must be designed. The relation between the applied field and the magnetization for a magnetic recording medium is given by the hysteresis loop. Such a relation is measured macroscopically by a vibrating sample magnetometer and only gives information about the average magnetic properties of the thin film. Parameters like H_c, M_r, S^*, OR, and S can be obtained from the loop and give characteristic information for recording media. Due to the small bit size in a medium it is also interesting to understand the magnetic characteristics on a small scale.

5. Preparation of Thin-Film Media

The general properties for media are a sufficient magnetization, M, for reading by the head with an acceptable S/N and an acceptable field strength to create a magnetization reversal directly related to the coercivity H_c. The latter parameter should not be too high for successful writing by the head field but it must be large enough to protect the medium against an unwelcome reduction of the signal during storing by demagnetization. For high density recording a significant potential for changing the signal during the required storing time is the self-demagnetizing field originated in the material itself and is proportional to the medium magnetization. Consequently the H_c must become higher for a more strongly magnetizable media and that is also the case if the recording density increases.

Based on the preparation technology and morphology two different types of recording media can be defined, namely, particulate-coated media and thin-film media. The first consists of discrete magnetic particles dispersed in organic resins and the second is created on the substrate (tape, floppy, hard disk) by depositing a continuous layer of a magnetic metal, alloy, or oxide. Although many different configurations have to be discussed for the different type of thin-film media used in the various fields of application, in general the essential design parts of such thin-film media are given in Figure 14. The media consists of a substrate made of glass, aluminum, polyester, etc; a transition (intermediate or seed layer) between the substrate and the magnetic (recording) layer; the magnetic layer(s); and a covering layer. They all consist of different materials, chemical compositions, microstructures, and thicknesses.

5.1. Thin-Film Media Preparation Technologies

A thin film can be defined as an area (volume) on top of a carrier (substrate) with properties differing from it. The interface between substrate and thin film has a great influence on the properties of the layer. The interface is determined by the properties of the substrate, the material(s) used for the thin film, and the method of deposition. During thin-layer processes the environment can be a liquid, gas, or vacuum. Such layers can be deposited by electro- or by electroless plating, chemical vapor deposition, and physical vapor deposition methods. A close relationship exists between deposition conditions, nucleation, and growth of the layer and their physical properties. Thin layers have properties that differ greatly from those of the bulk materials. These unique properties can be due to (*1*) their small thickness of a few atomic layers up to micrometer values, which, as a consequence, makes the surface/volume ratio of the layer completely different to that of the bulk; (*2*) because of their typical growth processes they are found in certain microstructures which are, in many cases, directly related to the physical properties; and (*3*) layer and substrate form a composite

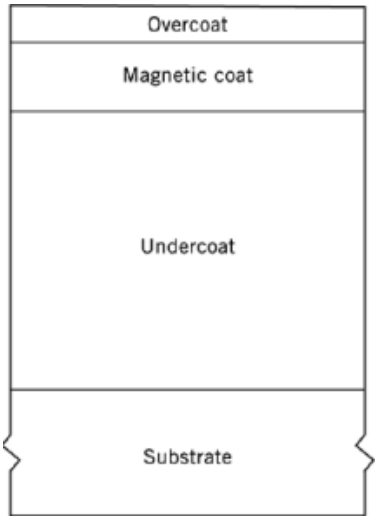

Fig. 14. Typical configuration of a thin-film media.

system resulting in a combination of properties based partly on the substrate properties and partly on the layer itself. By changing the deposition method and/or varying the different deposition parameters various layer structures and morphologies can be created over a wide range. The interaction between layer and substrate, ie, the interface, plays an important role by defining the structure and properties. In contrast to other fabrication methods it is possible to deposit solid materials which can have equilibrium as well as nonequilibrium properties. In the case of thin-film media for magnetic recording four deposition methods have been used, namely, electroless deposition, electrodeposition, vacuum evaporation, and sputtering. More information about deposition technologies and other properties of thin films in general can be found in the literature (38, 39).

Using the above-mentioned technologies, multilayers consisting of a few monolayers of ferromagnetic material alternating with a nonferromagnetic material can also be prepared. This technology is used for preparing media for magnetooptic recording and thin-film heads based on the magnetoresistance principle. The most important technologies used for preparing thin-film recording media will be discussed. Electrodeposition and autocatalytic plating (electroless deposition) were initially investigated in the early 1950s. The first magnetic disk for digital magnetic recording was introduced in 1960 and made by electrodeposition. Most of the media (ca 1993) are prepared by physical vapor deposition technologies such as evaporation and sputtering.

5.2. Vacuum Evaporation: Oblique-Incidence Deposition

Evaporation processes are usually carried out under vacuum within a pressure range of about 10^{-3} to 10^{-7} Pa ($10^{-5} - 10^{-9}$ torr). The various steps in the production of thin films with vacuum evaporation can generally be subdivided into the creation of the vapor-phase species, transport from source to substrate, and nucleation and growth on the substrate. The material flux is produced by the evaporation source which heats the material to the sublimation temperature: this can be done by resistance, radiation, eddy currents, electron and laser beams, etc. After evaporation the flux condenses on a cooler substrate. The low pressure is essential for having as few collisions as possible with the background gas species (a straight-line path) and a clean process. The emission characteristics of the source are discussed in detail in the literature. The growth speed on the substrate is not equal to the evaporation rate of the source and depends on the deposition

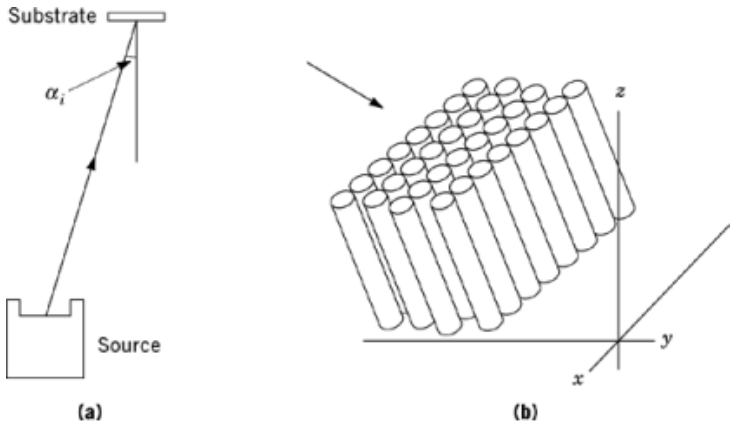

Fig. 15. Oblique-incidence evaporation (**a**) and a possible columnar structure (**b**).

geometry, the emission characteristics of the source, and the condensation coefficient in turn depending on the surface conditions and substrate temperature. Oxides, nitrides, etc, can be prepared by adding reactive gas during evaporation.

Because this method is important in relation to the preparation method of metal evaporated tape it will be discussed in more detail. The incidence angle of the atomic flux plays an important role in the nucleation and growth process. Atoms arriving under an angle at the substrate usually show a different behavior to those which approach perpendicularly. First of all, the shadowing effect plays an important role in the film formation. If there is no adatom (physically adsorbed atom) mobility and the sticking coefficient probability equals one, an incoming atom is captured as soon as it touches the substrate or surface atom. Atoms already deposited and surface irregularities throw a shadow. No direct impingement is possible in this shadowed area. When nonzero adatom mobility occurs, which is normally the case due to the kinetic energy of the atoms and the substrate temperature, they can then move to energetically favorable positions including the shadowed areas. Therefore, an increasing mobility partly annuls the shadowing effect. The degrees of shadowing and mobility are determined by the deposition conditions. The direction of the adatom movement is considered to have two contributors, namely surface diffusion (responsible for the movement in all directions), and the angle-of-incidence effect which causes the atoms to have a momentum component parallel to the incidence plane. This is true for the situation where the substrate is fixed in relation to the incoming flux.

The first paper about NiFe layers evaporated under an angle was published in the early 1960s (40). The films prepared this way are often called oblique-incidence or angle-of-incidence films. It was found that these kinds of films show an anisotropy whose strength depends on the angle of incidence of the atoms (α_i) during deposition (Fig. 15). If α_i is between 0 and 65 the anisotropy lies parallel to the film plane and perpendicular to the incidence plane.

Figure 15 gives an impression of the incidence angle of the evaporated flux and the final columnar structure. There is an anisotropic column aggregation perpendicular to the evaporation plane (yz-plane). The shadowing effect causes the columns to be separated by open regions. In the transverse direction (x-direction) there is a homogeneous distributed arrival of the atoms. The result is a higher packing density in the x- than in the y-direction. An explanation for the anisotropy based on the self-shadowing mechanism which means that a growing cluster of adatoms causes the shadowing of an adjacent region with respect to the vapor source has been given (40). Consequently, the film grows in chains (columns) oriented perpendicular to the plane of incidence. The shape anisotropy could be the reason for the macroscopic anisotropy. From a study of the effect of the mobility of metal atoms on the structure of oblique-incidence films the mechanism of inhibited mobility

was introduced (41). With this principle it is possible to give an explanation of the dependence of the preferred direction of growth of texture, angle of incidence, affinity of oxygen, substrate and source temperatures, melting point of the evaporated material, and background gas pressure. Other papers (42, 43) have stated that the shadowing mechanism alone is sufficient to explain the majority of the features of the microstructure. However, the modeling work in the papers used an atomic relaxation term which shows a strong resemblance to the mechanism of inhibited mobility. Most of the publications dealing with oblique incidence magnetic films have been produced by Japanese researchers, for example (44).

The relation between the columnar inclination angle (β) and the angle of incidence (α_i) of the evaporation flux was found to be $2\tan\beta = \tan\alpha_i$ (45). The so-called tangent rule is not always valid in a variety of experimental situations.

Besides columnar growth there is another aspect of the morphology, namely columnar bundling (46). Bundling is the growth of a column in the direction perpendicular to the evaporation plane. Bundling is also dependent on α_i, substrate temperature, deposition rate, and gas pressure, and bundling is even found in the direction of the evaporation plane. The interest in oblique-incidence thin films for magnetic recording purposes is mainly created by the experimental results that enable the magnitude and direction of the magnetic anisotropy, the coercivity, and a suitable squareness to be varied by modifying α_i. An overview paper has been published dealing with the oblique-incidence method especially when applied to perpendicuplar anisotropic thin films. The method consists of two opposite oblique sources which also makes it possible to tailor the chemical composition at the columnar boundaries (47).

5.3. Sputtering

From the physical point of view sputtering is a different process from vacuum evaporation. Generally the sputter deposition process implies the ejection of atoms from a target by energetic particles. The ejected atoms then condense on the substrate to form a thin film. The accepted theory of sputtering is based on a momentum transfer process. Therefore the sputtered atoms leave the target (source) with an appreciable kinetic energy (3–10 eV). A part of this energy is dissipated by collision processes with atoms of the sputtering gas. Upon arrival at the substrate the energy is still 1–3 eV whereas for vacuum evaporation it is smaller than 0.1 eV. Typical deposition rates are $0.5 - 50$ nm/s.

There are two principle sputtering methods, namely glow discharge sputtering and ion-beam sputtering. In the case of glow discharge sputtering (normally called sputtering) a glow discharge is formed between a negative anode (target) and the cathode (substrate holder) at earth potential. The anode potential is on the order of keVs. In the deposition chamber a so-called sputter gas (Ar, Xe, Kr) is admitted up to a pressure of about 1 Pa (10^{-2} torr) depending on the system and the type of sputtering.

The plasma is a partially ionized gas composed of electrons, ions, and a variety of neutral species. In principle the plasma is electrically neutral and the particles are uncontrollable. Interaction between the plasma particles and the substrate/film surface influences the growth. More information about sputtering can be found in the literature (48). Although there are many parameters which influence the final results of the layer such as the sputtering mode, the geometrical arrangements in the deposition unit (target/substrate distance, target size, substrate size), the type of targets (alloyed or multitarget), the most important sputter parameters are substrate temperature, argon pressure, and power. An overview of sputtering parameters, structural aspects, and the magnetic behavior of Co–Cr films for perpendicular recording is given (49).

5.4. Multilayer Technologies

During the 1970s and 1980s enormous advances in thin-film preparation processing have been made in the field of so-called artificial structuring of materials; semiconductors, metals, and insulators have been prepared in various sizes and geometries. Several classes of layered structures have been made using metal compounds.

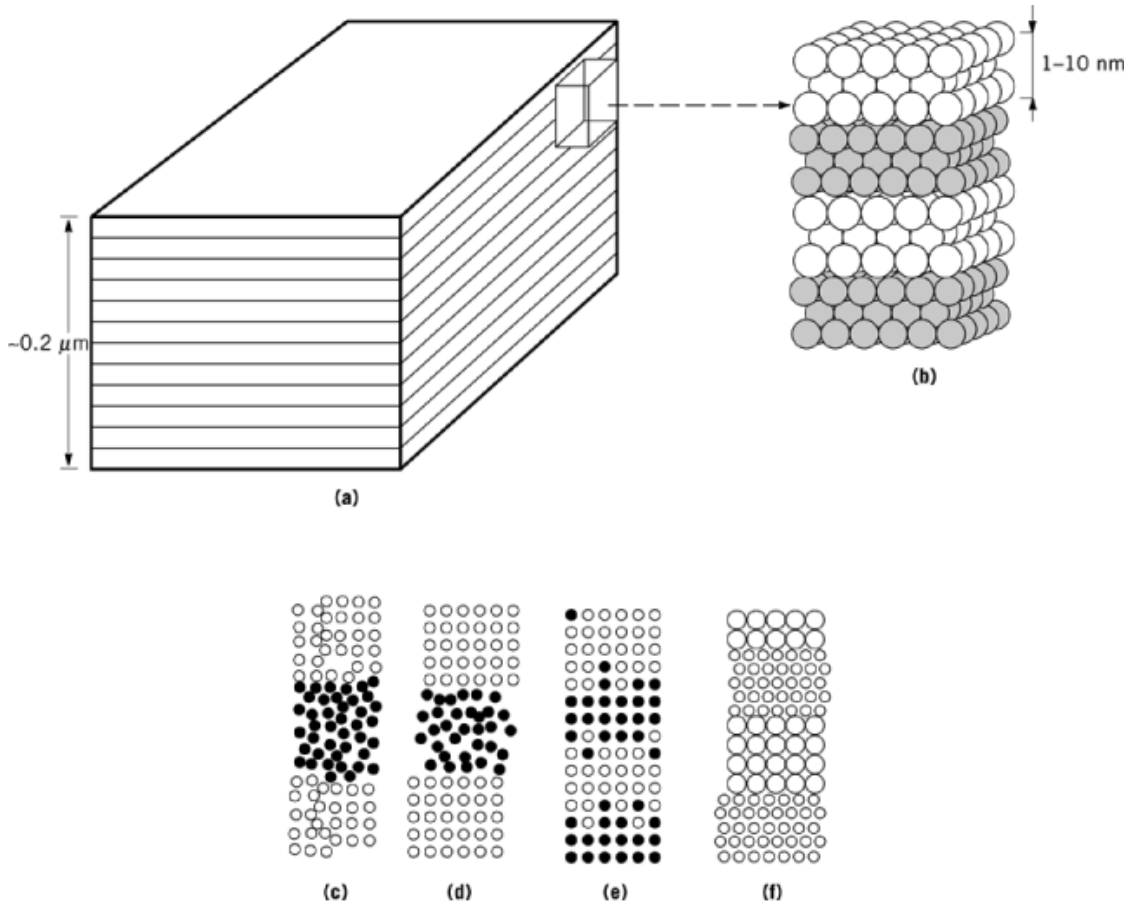

Fig. 16. Schematic presentations of the multilayer structure (**a**) and (**b**) and some different possibilities for stacking the individual thin layers (**c**–**f**).

Figure 16 shows a schematic representation of the various possibilities of obtaining structurally ordered multilayers. Generally, the total multilayer thickness (Fig. 16**a**) is in the tens of micrometer range whereas the individual layers (Fig. 16**b**) can be varied from one to tens of nm. Layered structures can be deposited by sequential depositing of two or more materials. After preparing a multilayered (metal) film, by alternating deposition of two elements, a periodicity alloy along the film normal should appear if the following conditions are satisfied: the layer thicknesses are determined on an atomic scale, a layered structure is formed, and the interdiffusion is sufficiently suppressed.

The choice of materials for metallic systems is still expanding and at present various examples of combinations with different atomic radii are being prepared. Here multilayered techniques also show possibilities for new material syntheses. In contrast to materials prepared by chemical procedures, superlattices are made far from equilibrium. The various possibilities for layering the artificial superlattice materials are given in Figure 1**c**–**f**. Most of the stacked layers (**c, d, f**) have more or less sharply defined boundaries and some have a noncrystalline structure in the individual layers (**c**) or one of the layers is noncrystalline (**d**). In such situations the structural information is not transmitted between adjacent layers and therefore, strictly speaking, no superlattice is formed. In the case of an unsharp boundary (**e**), compositionally modulated alloy-layered

structures have been made. The amplitude of composition modulation in the center of a layer can be in the range of 0 to 100%. Superlattices can also be formed with sharp boundaries ($<5\%$ of the thinnest layer) between the two components.

All these possible combinations strongly affect the electronic and physical properties of materials, especially when the dimensions of the layer structure become comparable with the characteristic lengths relevant to the properties in the particular materials. The application of multilayer structures in recording technologies plays an important role. Multilayer configurations are used in thin-film heads (magnetoresistance type) for magnetic recording as well as in media for magnetooptic recording. Crucial aspects important for these types of layers are the sharpness of the interface and the flatness. These aspects are strongly related to the method of preparation, the type of materials, and the substrates used. Generally speaking the layer growth mechanism plays the key role in the final interface structures.

6. Microstructure and Morphology of Thin-Film Media

The process parameters (flux rate, substrate temperature, etc), type of material (desorption, dissociation, and diffusion-energy terms), and the substrate properties influence the growth process. Depending on the process, film materials, and substrate behavior, all types of layer structures can be grown (amorphous, polycrystalline, and single crystal). Higher mobility of adatoms makes it possible to create films with deviating stoichiometry. Variations in substrate temperatures makes it even possible to deposit metastable structures. With treatment of the substrate surface or deposition of prenucleation centers it is also possible to grow films with a preferential crystallographic orientation (texture) and a specific morphology. A thin-film microstructure can be modified by means of substrate temperature, surface diffusion of the atoms, bombardment during film formation, incorporation of impurity atoms, and the angle-of-incidence effect of the incoming particle flux.

In most cases the final properties of the deposited layers differ principally from materials made by standard metallurgical methods. The substrate temperature is the most important process parameter for explaining the morphology of evaporated films (50). This result is modified for the sputtering process (51) and is extended with a second parameter, namely the argon pressure. In this work the influence of the surface roughness is also considerable. An impression of the structural features for sputtered films is given in Figure 17 called the Thornton diagram.

This zone-structure model has been revised (52) and accounts for the evolutionary growth stages of structure developments as well as the separate effects of thermally and bombardment-induced mobility. The reported experimental results between the microstructural aspects and deposition parameters should be used very carefully for personal results. Variation of the experimental parameters, using different types of materials, can result in divergent behavior. Generally, deposited thin films have higher defect densities than those of bulk materials. The defects in polycrystalline thin films are grain boundaries, column boundaries, voids, vacancies, dislocations, and interior gas bubbles. Defects are mostly responsible for the low temperature and interdiffusion processes. In the case of polycrystalline films the grain boundary is the most important detail. Epitaxial growth is a very special form of nucleation and growth and has a unique orientation relation with the substrate. Single-crystalline films can be prepared by the correct choice of the substrate material and deposition parameters.

6.1. Columnar Structure and Grain Size

Most of the deposited films reported in the literature have a so-called columnar structure (see Fig. 15). Depending on the substrate materials the columnar diameter can increase with the layer thickness or it is constant through the layer thickness. Further, the columnar diameter depends on the argon gas pressure during sputtering, the substrate temperature, and the bias voltage on the substrate. The method of deposition also has a large influence on the development of the columnar growth. In the case of Co-alloys deposited on polymer

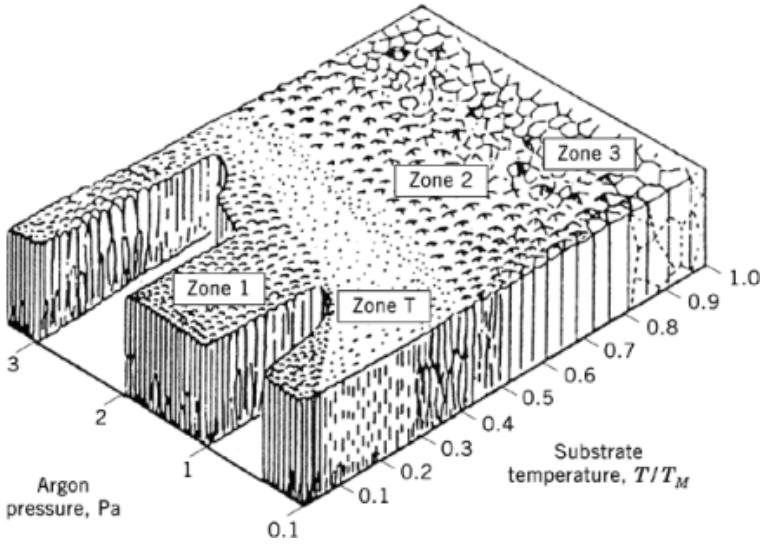

Fig. 17. Structural diagram (51) for sputtered layers. Zone 1 is a porous structure consisting of tapered crystallites separated by voids, Zone 2 shows columnar grains, and Zone 3 has a recrystallized grain structure. Zone T is a transition structure consisting of densely packed fibrous grains.

substrates extraordinary column or nodular growth is found. It can be seen from tem observations that the average crystal size has a 10–50 nm diameter. Depending on the preparation conditions the crystals can be mechanically separated (spacing about 4 nm) at the grain boundaries. Another separation of the crystals/columns is by segregated crystal boundaries with a nonferromagnetic material. This has been shown (53) in CoP plated disks. Grain size or columnar size are strongly influenced by the microstructure of the underlayer/substrate.

6.2. Crystal Structure and Texture

Many of the Co–X–Y thin-film media where X(=Cr, P) and Y(=Ta, Pt, Ni) do have a hexagonal close packed (hcp) structure with the texture axis (*c*-axis) parallel or perpendicular to the substrate surface depending on the properties of the Cr underlayer. It is also possible for the films to have fcc phases. The texture of a polycrystalline material can be simply defined as the crystallographic preferential orientation. In the case of a ferromagnetic thin film the orientation distribution of the column is of great importance because it determines the quality of the direction of the magnetic anisotropy. The texture axis should be perpendicular or in-plane oriented depending on the recording mode.

Another influence on the orientation is caused by the pressure of sputter gas and a worsening background pressure. It has been shown that a small amount of residual N_2 gas in the process chamber causes the formation of the fcc phase which also destroys the well-oriented hcp structure. Usually a higher Ar pressure means that the atoms are more scattered during their movement from target to substrate and consequently their kinetic energy is reduced. Therefore, for producing well-oriented ($\Delta\Theta 50 < 5$) films sputter equipment has to be optimized for certain process parameters. Data has been published on deposition of nonmagnetic underlayers or seed layers to improve the nucleation and growth of the Co–X–Y layers and increase the *c*-axis orientation.

6.3. Chemical Inhomogenities or Compositional Separation

Compositional separation at the grain boundaries influences the magnetic interactions of the individual grains. Deposition parameters such as temperature, substrate material, and the use of a seed layer play an important role. There are, in principle, two driving forces for obtaining the compositional separation, namely the temperature and deposition geometry.

Detailed studies of the chemical inhomogeneties in thin films for recording applications are seldom found. Most of the work that has been done has focused on Co–Cr media for perpendicular recording. Chemical separation of Cr in Co is very often called segregation, and this can be found at the column boundaries or even in the column itself. The boundary segregation is also described as oxygen gettering (54) which means that during the growth the Cr mainly reacts with oxygen; consequently the M_s of the magnetic composition increases. Another explanation is that there is a recombination of atoms, molecules, or clusters before they interact with the substrate (55). The formation of Cr–Cr and/or Co–Co clusters produces a compositional change. The same result can be obtained by using nonhomogenous targets (in the case of sputtering). Cr concentration on the lattice faults present in the column have been mentioned (56). Other explanations, where the Cr migrates to the boundary for thermodynamic reasons, can be found (57–59). These explanations are based on the fact that the Co–Cr system strives to attain a low as possible surface energy by the enrichment of the boundaries with Cr atoms because Cr has a larger surface than Co and also the binding energy is lower. The Cr atoms are exchanged with Co atoms at the surface and also at the column boundaries. The Cr distribution is dependent on deposition parameters such as temperature and energy of the incoming particles.

Often the phase diagrams of bulk Co–Cr systems have been used to explain the chemical composition although such a diagram is only valid at thermodynamic balance. A complete overview and new data have been published (60). With respect to the application of Co–Cr as a thin-film media for magnetic recording the most interesting area of the phase diagram is around the temperature range from room temperature to 1000°C. It can be seen from this phase diagram that at 35 at. % Cr and lower two hcp phases, one with a high Co-rich composition (ferromagnetic) and the other with a high Cr-rich content (paramagnetic) can exist. These phase diagrams are based on an equilibrium process and achieved from thermodynamic calculations. The thin-film materials discussed here are made by deposition which is by definition a nonequilibrium process. In studying these an important fact was assumed, namely that the phase diagram at high Co concentration below 800°C is very complicated because sluggish diffusion inhibits the equilibrium. It is known, for instance, that during sputtering the surface temperature of a grown film is quite different from that of the substrate (48). The bombardment exerted by various particles from the plasma on the surface results in a much higher temperature at the surface.

Most studies of the magnetic behavior of Co–Cr thin films have suggested that there is Cr segregation at the columnar boundaries which can explain the higher coercivity and the magnetic reversal behavior of the layers. However, only a few research groups have experimentally shown the existence of such a compositional separation. Nevertheless, the grain boundaries are assumed to be fast diffusion paths at which diffusion takes place by vacancies (61). Besides the segregation at the boundaries, Maeda (62) first introduced the so-called chrysanthemum-like pattern (CP model). This is also related to the thermal driving force. In this model the enhancement of Cr at the boundaries is a special case of the CP pattern (Fig. 18).

The CP structures are observed by tem but also in the case of very thick samples by sem (63). These kinds of observations are only possible in combination with selective etching techniques (64). Concentration fluctuations in the grains (columns) have also been studied by atom probe (65). These types of measurements can only be made after a special preparation technology of the Co–Cr film and substrate. The results show the atom–probe concentration depth in the planar direction of a Co–Cr column with an average composition of 22 at. % Cr. Over a depth of about 40 nm compositional differences of 30 at. % Cr and 7 at. % Cr have been measured. The latter composition is ferromagnetic whereas the composition above 26 at. % Cr is paramagnetic. The fluctuations are less than 10 nm. The main features of the CP structure are Co-rich stripes that tend to be perpendicular to

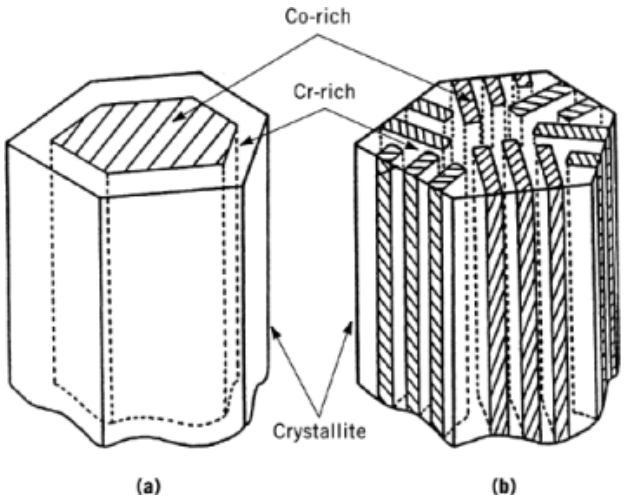

Fig. 18. Conventional segregated columns (**a**) and the CP structure (**b**).

the column boundaries. The CP structure also developed as a function of the thickness of the layer but mainly as a function of the substrate temperature. The Co-rich and the Cr-rich components strongly influence the magnetic properties. The spatial periodicity of compositional separation in sputtered Co–Cr layers on top of soft magnetic Ni–Fe layers is in the range of 3–7 nm (66). It has also been shown that compositional separation is present in Co–Cr–X materials used for longitudinal recording (67). Consistent results from experimental studies of field ion microscopy (fim), nuclear magnetic resonance (nmr), and transmission electron microscope (tem) in combination with etching techniques are presented.

6.4. Co Binary and Ternary Alloyed Thin Films

Most of the thin-film media for longitudinal and perpendicular recording consist of Co–X–Y binary or ternary alloys. In most cases Co–Cr is used for perpendicular recording while for the high density longitudinal media Co–Cr–X is used (X = Pt, Ta, Ni). For the latter it is essential to deposit this alloy on a Cr underlayer in order to obtain the necessary in-plane orientation. A second element combined with Co has important consequences for the Curie temperature (T_C) of the alloy, at which the spontaneous magnetization disappears. The T_C for Co is very high, 1131°C, and provides a reasonable margin for the amount of an additional element by which T_C usually decreases. It is also true, at least for bulk material, that adding Cr to Co can finally make the hcp structure become unstable and at certain compositions it is also possible that two crystal structures (fcc and hcp) are present. Furthermore it has been shown that even two different phases, one with a high Co-rich composition (ferromagnetic) and the other with a high Cr-rich content (paramagnetic) can be formed (68). Consequently, adding Cr to Co has two important effects; reduction of the T_C and M_s. For recording applications these values should be optimized. The T_C must not be too close to room temperature, because then the magnetic behavior becomes too sensitive for temperature variations. M_s should have a certain value because otherwise the information cannot be read by the head. The physics behind the reduction of M_s and T_C are complicated and not completely known. However, the most useful model when Cr is added to Co is to consider that the magnetic moment of Co atoms is reduced by electron transfer to its 3d band from Cr. It has been shown experimentally that the T_C drastically decreases with the Cr content and becomes paramagnetic just above about 22 wt % at room temperature. This is not expected if Cr only acts as a simple dilutant (69). Also, the transfer of 4s electrons from Cr to the 3d shell of Co may lower the magnetic moment (70). Furthermore, pure Cr is antiferromagnetic

at room temperature and a ferromagnetic sublattice coupling also seems to be an acceptable explanation for the relative strong decrease of T_C when compared with other X elements, which form an hcp phase with Co (71). Adding Cr to Co also gives an enhanced anisotropy field. Furthermore, with the variation of the Cr content it is possible to adjust H_c.

Another favorable influence on the film morphology is the reduction of the column dimensions (54) and the appearance of the compositional separation. The latter has a great influence on the magnetic microstructure because it can lead to more or less magnetically uncoupled columns if the enhancement of Cr at the column boundaries becomes higher than about 27 at. %. Smaller grain size has the advantage of a lesser surface roughness which results in a better head–medium interface. The choice of Cr also improves the corrosion resistance and mechanical hardness of the Co-based medium, although in a few cases other elements have been added to increase these properties. Also quaternary alloys Co–Cr–Pt–X ($X =$ Ta, B, Ni, B) have been reported (72, 73). The basic magnetic properties such as magnetization, coercivity, and anisotropy depend on the microstructural properties, compositional separation, and phase separation.

6.5. Surface Properties

In the case of very high density recording the surface becomes more and more important. On the one hand the surface smoothness and wearability are important because of the fact that the head–medium distance is very close and on the other hand for writing as well as reading the magnetic behavior is the key factor (74–77). Therefore, analyses of the chemical and structural properties (eg, surface topology) in relation to the magnetic properties are necessary. One conclusion is obvious, namely that for films with different surface and bulk hystereses, the magnetization cannot be homogeneous throughout the film thickness during all stages of the hysteresis curve. Therefore, this aspect should be studied in more detail because as film media are becoming still thinner, the surface volume ratio will be more important.

7. Microstructure and Magnetic Properties of Thin-Film Media

7.1. Magnetic Structure

An important characteristic of a medium is its magnetic structure, the magnetic unit (intrinsic domain structure or written bit) in the magnetizable layer which has, in principle, two oppositely stable directions parallel to the anisotropy axis. The switching of the magnetic units can be achieved by a sufficient applied field. Study of the magnetic structures and their switching behavior, etc, can be carried out by several techniques. The study of the M–H loop gives information about the macroscopic behavior of the media. Increasing density requires more knowledge about the micromagnetic behavior. More insight can be obtained by computer simulations (7). New experimental methods are available and being developed for collecting more information about the mesomagnetic (an area between macro and micro) properties of the media like the methods for observing the magnetic domains, domain walls, written bits, and stray fields using the Bitter-colloid sem method, magnetooptic Kerr (MO-Kerr) observations, Lorentz tem observations, electron holography, scanning electron microscope polarization analysis (sempa), anomalous hall measurements in combination with photolithography, and the magnetic force microscope (mfm).

The microstructure of the thin-film medium has a great influence on the magnetic behavior of the film. Is the magnetic behavior of the layer continuous or particulate? Both qualifications refer to the degree to which exchange forces are able to extend throughout the medium. In a continuous medium the exchange forces are hardly disturbed by structural discontinuities such as crystal boundaries. As a consequence the magnetic-domain boundaries then usually consist of Bloch line walls, which contain exchange and anisotropy forces. The typification particulate refers in the first instance to the method of preparation, whereby particles,

usually single-domain particles, are compounded together with nonmagnetic materials. In those media only the exchange forces are restricted to the volume of the particles, which therefore show only just magnetostatic interactions. Within this definition, from the magnetic point of view, it is possible that even thin films can be considered as particulate, showing distinct structural ferromagnetic units like crystals, columns, or clusters separated by nonferromagnetic materials or voids. Such kinds of microstructures can be influenced by the deposition methods and the nucleation and growth process of the layers. If the thin film has a continuous microstructure in which there is an exchange between the magnetic units, then at a remanent magnetic state (B_r in Fig. 2) the layer consists of magnetic domains having their direction of magnetization antiparallel and separated by a domain wall. The wall is a transition region in which the spins are rotated from one direction (domain A) in the other direction of domain B. The thickness of such a 180° wall is determined by minimizing the various energies and is, of course, dependent on the type of material (Co = 8.4 nm, Fe = 30 nm, and Ni = 72 nm).

The magnetization thin-film medium is strongly dependent on the microstructural properties. Depending on the morphology and chemical inhomogeneties of thin-film media the reversal take place as follows. Exchange coupled grains show a magnetic-domain structure which covers many grains and gives a reversal originated from domain-wall motion. The wall energy, influenced by crystalline anisotropy, magnetostatic energy at the wall, strain, chemical inhomogeneties, and film surface properties, dominates the coercivity H_c. Uncoupled grains which when reversed independently are, of course, influenced by magnetostatic interactions. Here the H_c is determined by crystalline anisotropy of the grain, shape, and strain anisotropy. Clusters of grains which are locally magnetically coupled can reverse in unison. These reversals are independent of other clusters, but again magnetostatic coupling can influence their behavior.

The shape of a magnetic material (sample geometry) is the most obvious feature which may influence the anisotropy. Depending on the geometry there is a magnetic charge at the surface of the uniformly magnetized sheet, cylinder, ball, or sphere. This magnetic pole density produces an internal uniform demagnetizing field $H_d(= -N_d M)$ which is, in fact, proportional to M and directed opposite to it. Here N_d is the linear demagnetizing factor. The sum of the three orthogonal vectors is equal to one ($N = N_x + N_y + N_z = 1$). The values for the three vectors depend on the shape of the magnetic unit. An important factor is that the magnitude of the internal field (H_{int}) is less than the applied field (H_{appl}) by the amount of the H_d. Consequently the H_{appl} must overcome the H_d in order to saturate the material.

7.2. Magnetization of Deposited Alloys

Frequently the relation between the magnetization and composition is presented by the Slater-Pauling curve which gives the relation between the saturation magnetization (M_s) and homogeneous bulk Co–X (78, 79). In general, most papers report that the M_s of sputtered and evaporated films, deposited at higher substrate temperatures, is found to be larger than that for bulk alloys having the same average chemical composition. Although in the literature various origins have been proposed, the most likely explanation is the phase separation. Two hcp phases, which hardly occur in bulk Co–Cr material at low temperatures, cause compositional fluctuations along the grain boundaries as the film growth proceeds.

Figure 19 compares experimental data with calculated curves (80). In the random Co–Cr alloy the Cr atoms are not distributed in the most suitable way for reducing the M_s of the alloy. Therefore the maximum local content of Cr for this distribution is much higher than in the case where Cr–Cr bonds are not present. The curve for no Cr–Cr bonds present shows that the M_s becomes zero at 25 at. % Cr, based on the fact that for bulk material the measured M_s for this composition is zero. Consequently 4 Cr nearest neighbor in an hcp lattice makes the final M_s zero.

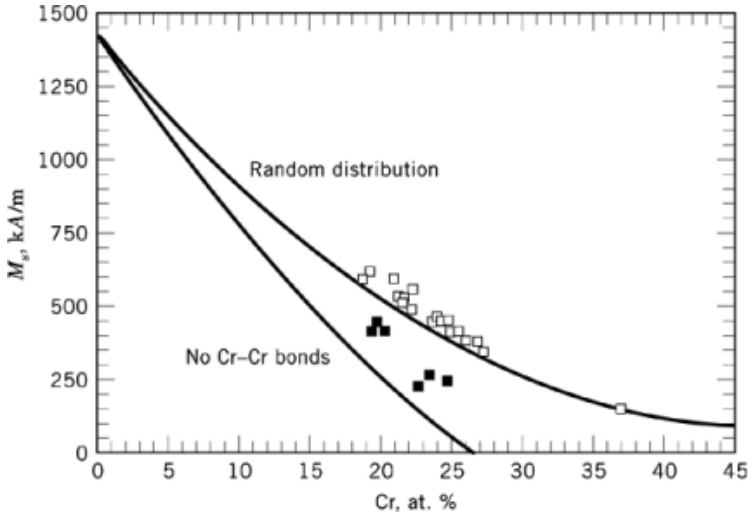

Fig. 19. M_s as a function of the Cr content in Co: (□), coevaporation at low temperature; (■), sputtered; and (—), calculated (80).

7.3. Coercivity of Thin-Film Media

The coercivity in a magnetic material is an important parameter for applications but it is difficult to understand its physical background. It can be varied from nearly zero to more than 2000 kA/m in a variety of materials. For thin-film recording media, values of more than 250 kA/m have been reported. First of all the coercivity is an extrinsic parameter and is strongly influenced by the microstructural properties of the layer such as crystal size and shape, composition, and texture. These properties are directly related to the preparation conditions. Material choice and chemical inhomogeneties are responsible for the M_s of a material and this is also an influencing parameter of the final H_c. In crystalline material, the crystalline anisotropy field plays an important role. It is difficult to discriminate between all these parameters and to understand the coercivity origin in the different thin-film materials in detail.

As has been seen in an ideal single-domain particle which switches coherently, the H_c is equal to the H_k if a field is applied in the easy axis direction. Depending on various factors, incoherent switching occurs and the H_c decreases. Even in a matrix of particles, with magnetostatic interaction the coercivity will again be influenced. Multidomain particles and thin films switch by domain-wall motion and again the coercivity decreases in comparison with the H_k. For many different morphologies the H_c is quite well described by the following general relation (81): $H_c = \alpha(2K_1/M_s) - N^*_{eff}M_s$ where N_{eff} = effective demagnetization factor. This relation gives a modification of the magnetocrystalline anisotropy and demagnetizing fields. The parameters α and N_{eff} relate to the microstructural aspects and the dimensions of the magnetic units. The influences of α and N_{eff} on the H_c for polycrystalline thin films have been discussed (82). In addition, for thin films surface and interface properties also influence the H_c. This leads to the assumption that the coercivity (an extrinsic property) can only be determined by means of the macroscopical hysteresis loop in combination with the theory of micromagnetism (83). Knowledge of the microstructural properties of the material cannot be omitted. In the first place the size and shape of the magnetic unit (crystal, column) material plays an important role. In single-domain particles the coercivity increases to a maximum at a critical particle-size diameter. Future increase of the diameter results in a multidomain-state particle. Decreasing the single-domain particle diameter it finally becomes superparamagnetic. At this stage H_c becomes independent of the diameter and the reversal takes place by thermal activation which again leads to a lower H_c. In the case of a multidomain particle the H_c is

determined by pinning mechanisms of the domain wall. These mechanisms are determined by the magnetically inhomogeneous regions like columnar boundaries, chemical inhomogenities, stacking faults, etc.

8. Thin-Film Media for Various Types of Recording

Thin-film media can be made by various technologies, eg, sputtered deposited Co–Cr–X films for longitudinal applications, laminated media for hard disk application, metal evaporated tape, and multilayers for possible applications in magnetooptic recording.

8.1. Sputtered Co–Cr–X/Cr Disks for Longitudinal Recording

Sputtered hard disks of Co–Cr–X ($X =$ Ni, Ta, Pt, C) for very high density longitudinal recording have been prepared and tested by many industrial and university groups. The first disks with a density larger than 1 Gbit/in.^{2} have been reported by IBM (13) and Hitachi (Japan) (16). The recording layers are deposited on a Cr underlayer which is deposited on the hard disk substrate. The composition is a Co ternary or quaternary composition and sputtering is the most favorable deposition technology for preparing these disks. The substrate consists of Ni:P plated on Al, glass, or canasite. The most important process parameters for depositing a suitable magnetic layer are the composition, thickness, and structure of the layer. The latter also depends on the structure of the Cr underlayer. The deposition parameters for both layers such as substrate temperature, bias voltage, and surface texture are also important.

8.1.1. Choice of Co–Cr

Sputtered Co–Cr films for perpendicular magnetic recording were first made at the Tohoku University in 1975 (84, 85). An overview of the preparation, microstructure, and magnetic properties of Co–Cr thin films has been given (49). Before Co–Cr was chosen, many different alloys of Co–*M* materials were investigated (86, 87), including $X =$ Rh, Pd, Mo, W, V, Ti, Cr, Mo, Pt, and Mn. All the Co–*M* films exhibit an hcp crystal structure with the *c*-axis oriented perpendicular to the film surface deposited on a variety of substrate materials. However if a Cr layer is used as seed layer (or buffer layer) then the Co–Cr start growing with an in-plane *c*-axis which is a condition for longitudinal recording. For further tailoring longitudinal media, ternary and quaternary alloys have been prepared and used as high density media (14, 16).

8.1.2. Role of the Cr Underlayer

One of the methods to overcome the problem of low coercivity in vacuum evaporated films is an underlayer between the substrate and the ferromagnetic layer, which was already proposed in 1967 (88). By slow deposition (0.1 nm/s) of a Co layer (thickness less than 100 nm) on a Cr underlayer with bcc structure the coercivity increases at a level suitable for magnetic recording. The H_c is strongly dependent on the rate of deposition, the thickness of the Co as well as the Cr layers, and the substrate temperature. The Cr underlayer induces the growth of the Co layer with an exclusive hexagonal crystalline structure and a narrow crystallite-size distribution. If the Cr layer increases, its crystal size also increases and the Co grows more quasiepitaxial. The *c*-axis orientation of the Co becomes more in-plane if the substrate temperature increases. An important fact is that this effect is strongest if the deposition of the Co occurs immediately after the deposition of the Cr underlayer (no oxidation). The role of the Cr underlayer is thus the creation of the right conditions for epitaxial growth of the polycrystalline layer having the hcp texture *c*-axis in the plane of the medium. Optimizing the Cr layer also controls the crystal size and morphology. It was reported in 1986 (89, 90) that the Cr underlayer thickness has a great influence on the coercivity of the Co–Ni–Cr layer. In most of the literature it can be found that with increasing Cr thickness the H_c increases. Under ideal conditions and the right material combinations coercivities above 240 kA/m have been prepared.

8.1.3. Randomly In-Plane Texture

The *c*-axis orientation is important for the magnetic anisotropy. The Co-based alloys used mostly have an hcp structure with the *c*-axis randomly in-plane, but it is also possible to create a tilted *c*-axis depending on the underlayer structure (91). On thick Cr underlayers the (10.1) Co–Cr–Ta orientation growth on the Cr (100) plane finally leads to a tilted *c*-axis of 28° with respect to the substrate plane, but, for instance, the (11.0) of Co–Cr–Pt layers grow epitaxially on the Cr (100) resulting in a *c*-axis orientation of the magnetic layer in-plane. An optimized Cr thickness is found for this type of epitaxial growth. Much research will have to be carried out before a complete understanding of this type of growth can be obtained.

8.1.4. Oriented In-Plane Texture

In this kind of film the properties (H_c and M_r) in the various in-plane directions (texture and nontexture directions) are different. The texture of the film can be supported by the texture of the substrate and the crystal lattice can be smaller in the texture direction than in the transverse direction. This can be the source for strain-induced magnetic anisotropy (magnetostriction). It is also found that the crystal is aligned in the texture direction (92).

8.1.5. Morphology

Thin films should magnetically operate as individual particles. The exchange between the crystals should be broken or at least minimized. This can be realized by mechanical separation or by segregated crystal boundaries with nonferromagnetic compositions. The Cr underlayer is responsible for the physical separation. Cr grows with a columnar morphology and has a rough surface structure (93). It was reported that the dome-like surface roughness is on the order of tens of nm depending on the thickness of the Cr layer. It can be observed from tem observations (13) that in combination with a high Ar sputter-gas pressure the Co–Cr–Pt layer shows physically separated crystal boundaries.

8.1.6. Compositional Separation

Similar effects as shown for Co–Cr films used for the perpendicular recording mode compositional separation also occurs in Co–Cr–X films for longitudinal recording, although at present only limited experimental data is available. Most data from in-plane media is derived from macroscopic magnetic measurements, which on Co–Cr–Ta showed that an increase in Ta content also increases the magnetization and suggests that this effect is due to increasing the Cr segregation at the boundaries. Another effect by applying Ta is the increase of the lattice constant which leads or reduces strain in the lattice, and it was suggested that this influences the H_c. In Co–Cr–Pt it was found that the increase of the lattice constant can be correlated with the increase of H_c. The Pt in these types of ternary alloys can also play a role by the formation of the very hard $Co_{50}Pt_{50}$ composites which have a large influence on the reversal behavior.

8.2. Laminated Hard Disk Media

Many studies have been published on thin-film media consisting of more magnetic layers separated by a nonferromagnetic interlayer (94–98). The main aim for studying the laminated medium structures for high density recording is to improve the signal-to-noise ratio by reducing the medium noise. The linear density is determined by the macroscopic magnetic properties H_c and remanence thickness product $M_r\delta$ while the medium noise is related to the individual grain structure and the exchange coupling between the grains.

Individual control of the parameters H_c and the $M_r\delta$ in thin films was announced in 1979 (99) proposing stacked Co-films. The increase of H_c and $M_r\delta$ in a four-layer system consisting of a Cr underlayer (300 nm)/CoNiCr (35 nm)/Cr interlayer (12.5 nm)/CoNiCr (35 nm) have shown better read/write characteristics (100). It has also been reported that the noise contribution in such a system can be reduced because the noise of the individual layers is lower than that of a thicker single layer (96). The total noise is the sum of the noise of

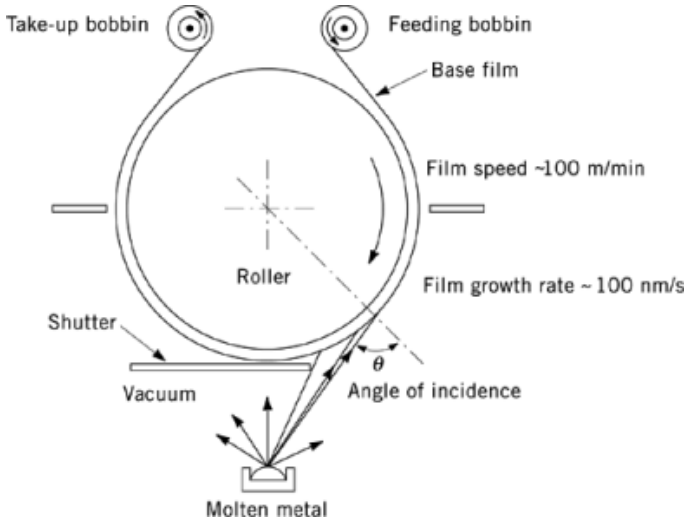

Fig. 20. Mass-production equipment for metal evaporated tape (103); vacuum ~1 mPa (10^{-} torr).

the individual two layers plus a cross term. The key is now to design individual layers with low noise behavior. One of the advantages of the laminated technology is that the growth of the magnetic layer is interrupted in an early stage which gives a better opportunity to obtain uncoupled (exchange) crystals. This research is in progress by using a variety of materials and deposition parameters. An important aspect is that the interlayer thickness should be thick enough for interrupting the exchange between the magnetic layers but thin enough to keep magnetostatic coupling. In comparison with the common technologies the manufacturing control of macromagnetic and micromagnetic properties is more difficult in the laminated process (101).

8.3. Metal Evaporated Tape

Very pure films and to a certain extent preselected structures and morphologies can be obtained by vacuum evaporation. Atoms and molecules are emitted from the sources by heating and exist in a gaseous state. The pressure in the vacuum chamber, a certain equilibrium pressure (saturated-vapor pressure), is established at a given temperature. The deposition rate (R) depends on the vapor pressure. The best results can be obtained if the evaporated elements and their alloys have a similar vapor pressure, but this is a limitation of the method. In the case of deposition of Co–Ni as a recording media this problem is not present. There are two methods to overcome the low H_c by evaporation, namely a Cr underlayer and deposition by varying the angle of incidence of the arriving metal atoms (102).

In order to produce the so-called ME (metal evaporated) tape, modifications relative to the oblique incidence evaporation have been made in order to obtain efficient use of the evaporated material and continuous evaporation over the total length of the substrate, ie, hundreds of meters of tape have to be produced in one single run at a very high production speed (Fig. 20). The most important modification is that the evaporation occurs over a range of angles, instead of one angle, whereby the incidence angle changes as the substrate passes along the vapor beam. This means that the direction of the elongated columns changes throughout the thickness of the tape. The properties of continuous varied incidence Co, Ni, Co–Ni, and Fe tapes have been investigated (103).

A principle deposition geometry is given in Figure 20. Depending on the rotation direction of the substrate (tape) two nucleation processes can take place, namely HIN and LIN. In high incidence-angle nucleation (HIN)

Fig. 21. Transmission electron micrograph (tem) made from a cross-section of a metal-evaporated tape medium with the typical banana-like shape of columns. The layer thickness is $\sim$120 nm.

the nucleation takes place at high incoming angles of the beam and successive growth occurs with a decreasing incidence angle. In low incidence-angle nucleation (LIN) the nucleation starts at low incidence angles and further growth occurs with an increase of the incidence angle. But at such a high angle of incidence the incoming vapor beam is almost parallel to the substrate and the deposition rate becomes very low. In addition the packing fraction is strongly reduced.

Last but not least the corrosion resistance of this type of material is very poor. A partly oxidized medium is the solution; therefore during deposition oxygen was added. The final composition of Co–Ni–O also gave the right magnetic medium properties. The H_c is strongly influenced by the O_2 value.

The morphology of the ME tape can be seen in Figure 21. In the cross-sectional microstructure, prepared by ion milling, the so-called banana-shaped morphology is clearly visible. Due to the shadowing effect the density of such a film is not high and the micromagnetic behavior is probably a mixture of domain-wall motion and rotation of the magnetization. The structural analysis of the tape provides the following data. The thickness of the magnetic layer is about 130 nm and a regular structure composed of very fine fibers is observed (thickness 3–10 nm). The columns make an angle of 37° relative to the plane of the film. Auger electron spectroscopy (aes) has shown an average composition of $Co_{77}Ni_{10}O_{13}$ (104, 105).

The substrate side seems to be less dense which is to be expected from large shadowing at a high incidence angle. It is anticipated that the fiber-like structure consists of crystallites. An hcp Co phase as well as a Ni–O fcc phase were found by x-ray diffraction. The anisotropy of such a complicated composition has been analyzed (106) and a correlation between the anisotropy direction and pulse shape have also been analyzed (105). The angle of incidence method has also been used for a hard disk preparation (107). Two electron gun sources were used and the evaporated beam was deposited under an angle of 60° on both sides of the rotatable-disk substrate. The material used was $Fe_{42.5}Co_{42.5}Cr_{15}$ and was deposited on a substrate of Al–Mg with an underlayer of stainless steel which needs a special treatment to create the right surface structure of the magnetic layer to prevent adhesive contact between the head and the medium.

8.4. Multilayers for Magnetooptic Recording

In 1957 the first MO medium, a thin film of MnBi, was proposed and based on the principle of Curie temperature writing. Later MnAlGe and CoPt were intensively studied followed by GdCo, but this material was used for compensation-point writing. None of the materials was ideal; for instance MnBi consists of two crystallographic phases and is very unstable above 400°C. The noise problem was high in the case of MnAlGe media and domain instability played the most important role in the case of GdCo.

Magnetooptic materials have been selected on the basis that they can sustain submicrometer domains, have a large signal-to-noise ratio supported by sufficient magnetooptic effects, and are resistant to corrosion and have chemical stability. The most popular materials at the present time are the amorphous rare-earth (Gd, Tb, and Dy) transition-metal (Fe, Co) alloys which are deposited by evaporation or sputtering alloys like

GdTbFe and TbFeCo are well known and can be made commercially. There is a great interest in and a great deal of research on so-called multilayer structures (see Fig. 16) for MO applications (108).

Mainly Co–Pt and Co–Pd have been studied by evaporation and sputtering. Although both processes show different physical processes the MO properties of the films do not vary much. Studies have also been carried out for materials with a lower Curie temperature (109).

9. Conclusions

Particulate recording media have been prepared with success since the 1950s although they have shown disadvantages. Thin-film hard disk materials are attracting great interest for ultrahigh density recording either for longitudinal or perpendicular modes. There is a trend to use more and more thin-film heads; also, the MR head is used for many high density recording set-ups. Ternary and quaternary Co–Cr–X–Y alloys have been proposed as suitable media for longitudinal high density thin-film media. Underlayers (mostly Cr) are necessary for controlling the magnetic properties. Higher density in longitudinal recording needs thinner layers and smaller crystallites. A trend is that the layer thickness for hard disk application must decrease to about 10–15 nm for obtaining 10 Gbit/in.^{2} density recording. Thin-film materials are also essential for magnetooptic applications, and an increase in densities can also be expected from the various multilayers developed so far.

The microstructure and morphology is important for the new class of high density recording media. Magnetic properties which should be optimized are the coercivity, the remanence-thickness product ($M_r\delta$), and the S^*. The sharpness and shape of the written transition is determined by the grain morphology, magnetical discoupling of the grains, and their textures. The higher M_r and lower δ for obtaining ultimate density will be finally limited by the superparamagnetism. High coercivity and low noise media are required for longitudinal recording. In the case of the perpendicular mode of recording optimization has to be carried out for the normalized-particle coercivity distribution as proposed in Reference 110.

A trend from the history of the high density recording technology shows that the recording density has increased by a factor 10^3 since the 1960s. Densities of 10 Gbit/in.^{2} for hard-disk applications and several bits/μm for tape application, are part of long-term planning. With respect to perpendicular recording, high linear-bit densities have been demonstrated on laboratory scale, achieved by recording a medium consisting of Co–Cr–Ta on a soft magnetic underlayer with a special single-pole head (111). In the case of pmr the ultimate densities of bit areas (2500 nm^2) are predicted with bit lengths smaller than 50 nm (10).

BIBLIOGRAPHY

Cited Publications

1. C. D. Mee and E. D. Daniel, *Magnetic Recording*, Vols. **1**–**3**, McGraw-Hill Book Co., Inc., 1987–1988; and updated ed., *Magnetic Recording Handbook, Technology and Application*, 1990.
2. A. S. Hoagland and J. E. Monson, *Digital Magnetic Recording*, 2nd ed., John Wiley & Sons, Inc., New York, 1991.
3. R. M. White, ed., *Introduction to Magnetic Recording*, IEEE Press, New York, 1985.
4. J. C. Mallinson, *The Foundations of Magnetic Recording*, 2nd ed., Academic Press, Inc., London, 1993.
5. K. H. J. Buschow and co-workers, eds., *High Density Digital Recording*, Kluwer Academic Publishers, Series E: Applied Sciences-Vol. **229**, NATO ASI series, Dordrecht, the Netherlands, 1993.
6. T. C. Arnoldussen and co-workers, eds., *Noise in Digital Magnetic Recording*, World Scientific Publishing Co., Singapore, 1992.

7. H. N. Bertram in J-G. Zhu, in H. Ehrenreich and D. Turnbull, eds., *Solid State Physics*, 46, Academic Press, Inc., San Diego, 1992, 271–371.
8. B. Bhushan, *Tribology and Mechanics of Magnetic Storage Devices*, Springer-Verlag, New York, 1990.
9. H. N. Bertram, *Theory of Magnetic Recording*, Cambridge University Press, Cambridge, U.K., 1994.
10. Y. Nakamura, *J. Magn. Soc. Jpn.* **15**(52), suppl., (1991).
11. I. Tagawa and Y. Nakamura, *J. Magn. Soc. Jpn.* **13**(S1), 97 (1989).
12. E. S. Murdock, R. F. Simmons, and R. Davidson, *IEEE Trans. Magn.* **28**, 3078 (1992).
13. T. Yogi and co-workers, *IEEE Trans. Magn.* **26**(5), 2271 (1990).
14. C. Tsang and co-workers, *IEEE Trans. Magn.* **26**, 1689 (1990).
15. T. D. Howell and co-workers, *IEEE Trans. Magn.* **26**, 2298 (1990).
16. M. Futamoto and co-workers, *IEEE Trans. Magn.* **27**, 5280 (1991).
17. M. L. Williams and R. L. Comstock, *AIP Conf. Procs.* **5**, 378 (1971).
18. D. B. Richards and T. J. Szczech, *J. Appl. Phys.* **49**(3), 1819 (1978).
19. E. Koster, H. Jakusch, and U. Kullmann, *IEEE Trans. Magn.* **17**(6), 2250 (1981).
20. T. Suzuki, *IEEE Trans. Magn.* **20**(5), 675 (1984).
21. S. Iwasaki and K. Tekamura, *IEEE Trans. Magn.* **11**, 1173 (1975).
22. E. Katz and P. Schreiber, *J. Magn. Soc. Jpn.* **15**(S1), suppl., 483 (1989).
23. H. Hamilton, *J. Magn. Soc. Jpn.* **15**(S2), suppl., 483 (1991).
24. Proceedings of the PMRC '89, *J. Magn. Soc. Jpn* **13**(S1), suppl., more than 900 pages (1989), and Proceedings PMRC '91, *J. Magn. Soc. Jpn.* **15**(S2), suppl., more than 1000 pages (1991).
25. S. Iwasaki, Y. Nakamura, and K. Ouchi, *IEEE Trans. Magn.* **15**, 1456 (1979).
26. T. Suzuki, *IEEE Trans. Magn.* **20**, 675 (1984).
27. C. Kooy and U. Enz, *Philips Res. Repts.* **15**, 7 (1960).
28. H. J. Williams and co-workers, *J. Appl. Phys.* **28**, 1181 (1957).
29. F. J. A. M. Greidanus, *Philips J. of Res.* **45**, 19 (1990).
30. W. Bas Zeper, *Magneto-optical Recording Media on Co/Pt Multilayers*, Ph.D. dissertation, University of Twente, Enschede, the Netherlands, 1991.
31. W. Reim, J. Schoenes, and P. Wachter, *IEEE Trans. Magn.* **20**, 1045 (1984).
32. A. Aharoni, *IEEE Trans. Magn.* **22**, 478 (1986).
33. E. Stoner and E. P. Wohlfarth, *Philos. Trans. R. Soc. Lond. Ser. A* **240**, 74 (1948).
34. I. S. Jacobs and C. P. Bean, *Phys. Rev.* **100**, 1060 (1955).
35. C. P. Bean, *J. Appl. Phys.* **26**(11), 1381 (1955).
36. S. D. Cullity, *Introduction to Magnetic Materials*, Addison-Wesley, Reading, Mass., 1972, 399–418.
37. T. Wielinga, J. C. Lodder, and J. Worst, *IEEE Trans. Magn.* **18**, 1107 (1982).
38. R. F. Bunshan and co-workers, *Deposition Technologies for Films and Coatings*, Noyes Data Corp., Park Ridge, N.J., 1982.
39. L. I. Maisel and R. Clang, eds., *Handbook of Thin-Film Technology*, McGraw-Hill Book Co., Inc., New York, 1970.
40. D. O. Smith, M. S. Cohen, and G. P. Weiss, *J. Appl. Phys.* **31**, 1755 (1960).
41. J. G. W. van De Waterbeemd and G. W. Van Oosterhout, *Philips Research Reports* **22**, 375 (1967).
42. A. G. Dirks and H. J. Leamy, *Thin Solid Films* **47**, 219 (1977).
43. A. G. Dirks and H. J. Leamy, *J. Appl. Phys.* **49**(6), 2430 (1978).
44. H. Fujiwara and co-workers, *Thin Solid Films* **163**, 387 (1988).
45. J. M. Nieuwenhuizen and H. B. Haanstra, *Philips Tech. Rev.* **27**(1), 87 (1966).
46. S. Keitoku, *J. Sci. Hiroshima Iniv., Ser A* **37**(2), 167 (1973).
47. H. Van Kranenburg and J. C. Lodder, *Mat. Sci. Eng. Rep.* **R11**(7), 295–354 (1994).
48. B. Chapman, *Glow Discharge Processes*, John Wiley & Sons, Inc., New York, 1980.
49. J. C. Lodder, in K. H. J. Buschow and co-workers, eds., *High Density Recording*, NATO ASI Applied Sciences-vol. **229**, Kluwer Academic Publishers, Dordrecht, the Netherlands, 1993, Chapt. 6, 59–99.
50. B. A. Movchan and A. V. Demschishin, *Phys. Met. Metallogr.* **28**, 83 (1969).
51. J. A. Thornton, *Am. Rev. Mater. Sci.* **7**, 239 (1977).
52. R. Messier and co-workers, *J. Vac. Sci. Techn.* **A2**(2), 500 (1984).
53. M. Aspland, G. A. Jones, and B. K. Middleton, *IEEE Trans. Magn.* **5**, 314 (1969).

54. J. Smits, S. B. Luitjens, and F. J. A. den Broeder, *J. Appl. Phys.* **55**(6), 2260 (1984).
55. A. K. Jinghan, *J. Magn. Magn. Mater.* **54–57**, 1685 (1986).
56. U. Hwang and co-workers, *Thin Solid Films* **147**, 231 (1987).
57. J. N. Chapman, I. R. McFadden, and J. P. C. Bernards, *J. Magn. Magn. Mater.* **62**, 358 (1986).
58. M. Sagoi, R. Nishikawa, and T. Suzuki, *IEEE Trans. Magn.* **22**(5), 1335 (1986).
59. F. F. Abraham and C. R. Bundle, *J. Vac. Sci. Techn.* **18**(2), 506 (1981).
60. K. Ishida and T. Nishizawa, *Bull. Alloy Phase Diag.* **11**, 357 (1990).
61. N. L. Peterson, *J. Vac. Sci. Techn. A* **4**(6), 3066 (1986).
62. Y. Maeda, S. Hirono, and M. Asahi, *Jpn. J. Appl. Phys.* **24**, L951 (1985).
63. Y. Maeda and co-workers, *J. Magn. Soc. Jpn.* **15**(S2), suppl., 457 (1989).
64. Y. Maeda and M. Asahi, *J. Appl. Phys.* **61**(5), 1972 (1987).
65. K. Hono and co-workers, *Appl. Phys. Lett.* **62**, 2504 (1993).
66. Y. Maeda and co-workers, *J. Magn. Soc. Jpn.* **15**(S2), 457 (1991).
67. Y. Maeda and K. Takei, *J. Magn. Soc. Jpn.* **16**(2) (1992).
68. K. Ishida and T. Nishizawa, *Bull. Alloy Phase Diag.* **11**, 357 (1990).
69. T. Wielinga, *Investigations on Perpendicular Recording*, Ph.D. dissertation, University of Twente, Enschede, the Netherlands, 1983.
70. J. A. Aboaf and E. Klokholm, *IEEE Trans. Magn.* **17**(6), 3160 (1981).
71. K. Kobayashi and G. Ishida, *J. Appl. Phys.* **52**(3), 2453 (1981).
72. T. Yamashita and co-workers, *IEEE Trans. Magn.* **27**, 4727 (1991).
73. C. R. Paik and co-workers, *IEEE Trans. Magn.* **28**(5), 3084 (1992).
74. O. Lopez and D. A. Clark, *J. Appl. Phys.* **57**(1), 3943 (1985).
75. O. Lopez and D. A. Clark, *IEEE Trans. Magn.* **21**(5), 1401 (1985).
76. Y. Nakamura, *J. Magn. Soc. Jpn.* **13**(S1), 33 (1989).
77. W. J. M. A. Geerts, J. C. Lodder, and Th. J. A. Popma, *J. Magn. Magn. Mat.* **104–107**, 971 (1992).
78. R. M. Bozorth, *Ferromagnetism*, Van Nostrand, New York, 1951, p. 441.
79. J. C. Slater, *J. Appl. Phys.* **8**, 385 (1937), and L. Pauling, *Phys. Rev.* **54**, 899 (1938).
80. W. G. Haines, *J. Appl. Phys.* **55**(6), 2263 (1984).
81. H. Kronmueller, *Phys. Stat. Sol.(b)* **144**, 385 (1987).
82. H. Kronmueller, *J. Magn. Soc. Jpn.* **17**, 260 (1993).
83. W. F. Brown, *Micromagnetics*, Wiley-Interscience, New York, 1963, p. 75.
84. S. Iwasaki and H. Yamazaki, *Proc. of the 7th Conf. on Magn. Soc. Japan*, 4pA-7, (1975), in Japanese.
85. S. Iwasaki and K. Ouchi, *IEEE Trans. Magn.* **14**, 849 (1987).
86. S. Iwasaki, K. Ouchi, and N. Honda, *IEEE Trans. Magn.* **16**(5) (1980).
87. K. Kobayashi and G. Ishida, *J. Appl. Phys.* **52**(3), 2453 (1981).
88. J. P. Lazzari, I. Melnick, and D. Randet, *IEEE Trans. on Magn.* **3**(3), 205 (1967).
89. G. Chen, *IEEE Trans. Magn.* **22**, 334 (1986).
90. M. Ischikawa, *IEEE Trans. Magn.* **22**(5), 573–575 (1986).
91. G. E. Johnson and co-workers, *J. Appl. Phys.* **67**, 4686 (1990).
92. J. M. Simpson and co-workers, *IEEE Trans. Mag.* **23**, 3405 (1987).
93. S. Agarwal, *IEEE Trans. Magn.* **21**, 1527 (1986).
94. S. E. Lambert and co-workers, *IEEE Trans. Magn.* **29**(1), 223–229 (1993).
95. S. E. Lambert, J. K. Howard, and I. L. Sander, *IEEE Trans. Magn.* **26**(5), 2706–2708 (1990).
96. E. S. Murdock, B. R. Natarajan, and R. G. Walmsley, *IEEE Trans. Magn.* **26**(5), 2700 (1990).
97. H. T. Hata and co-workers, *J. Appl. Phys.* **67**, 642 (1990).
98. D. C. Palmer and co-workers, *IEEE Trans. Magn.* **27**, 307 (1991).
99. W. T. Maloney, *IEEE Trans. Magn.* **15**(3), 1135 (1979).
100. S. Katayama and co-workers, *IEEE Trans. Magn.* **24**(6), 2982–2984 (1988).
101. K. E. Johnson and co-workers, *IEEE Trans. Magn.* **29**(1), 215 (1993).
102. D. E. Speliotis and co-workers, *J. Appl. Phys.* **36**, 972 (1965).
103. K. Nakamura, Y. Ohta, and A. Itho, *IEEE Trans. Magn. Mag.* **18**, 1077 (1982).
104. J. S. Gau and co-workers, *J. Appl. Phys.* **61**(8), 3807 (1987).

105. G. Krijnen and co-workers, *IEEE Trans. Magn.* **24**(2) (1988).
106. S. Swaving and co-workers, *J. Magn. Magn. Mater.* **67**, 155 (1987).
107. T. C. Arnoldussen and co-workers, *IEEE Trans. on Magn. Mag.* **20**, 821 (1984).
108. C. J. Robinson, T. Suzuki, and C. M. Falco, eds., *Materials for Magnet-Optic Data Storage*, Materials Research Society Proceedings 150, Pittsburgh, Pa., 1989.
109. M. Mes and co-workers, *J. Magn. Soc. Jpn.* **17**, 44–47 (1993).
110. K. Tagawa and Y. Nakamura, *IEEE Trans. Magn.* **27**(6), 4975 (1991).
111. Y. Nakamura and H. Muraoka, *IEEE Trans. Magn.* **27**, 4555 (1991).

J. C. LODDER
University of Twente

Related Articles

Information Storage Materials, Optical; Thin films